

Nonlinear Plasma Science

Some Recent Results and State of the Art

Yannis Kourakis

Khalifa University of Science and Technology, Abu Dhabi, UAE

IoannisKourakisSci@gmail.com , ioannis.kourakis@ku.ac.ae

Collaboration with:

Mehdi Jenab (Canada), Amar Kakad (India), Shahid Ali (Pakistan),
Sebastien Guisset (CEA, France), Michael McKerr (Belfast, UK), Ibrahem Elkamash (Egypt),
Manfred A. Hellberg (South Africa), Frank Verheest (Belgium), Vikrant Saxena (India)

Special thanks: Mark Dieckmann (Sweden), Amaria Javed (UAE), Jad Bassous (UAE)

Acknowledgment: ASPIRE ex. ADEK – Abu Dhabi Education & Knowledge council (AARE grant ADEK/HE/157/18)

Khalifa University internal funding via project FSU-2021-012 / 8474000352.

Regional E-conference on Physics (part of the IUPAP centennial celebration), Pakistan, 18th -21st January 2022

Layout

- 1. Historical background and basics
 - 2. Overview of current trends and frontier topics:
 - Electrostatic Solitary Waves (ESWs)
 - Supersolitons
 - Phase-space holes
 - Freak waves
 - 3. Summary, discussion, conclusions
-

Nonlinear excitations - *Solitary waves (SWs)*

- SWs occur in abundance in Nature, in various physical contexts
- are ***localized coherent structures***, bearing remarkable properties: preserve their shape (stationary profile), are robust, i.e. persist against perturbations and collisions with one another, ...
- represent localized lumps of energy, whose manifestation may be constructive (e.g. signal transmission) or destructive (*tsunami*)
- bear various generic forms and names: ***pulses, kinks, holes, shocks, double layers*** or ***potential dips*** (in plasmas), ...
- may either be non-periodic forms (e.g., pulses) or may possess a quasi-periodic internal structure (e.g., oscillons, envelope pulses, breathers)

Solitary waves crossing on a beach



Ocean solitons east of the Strait of Gibraltar



Internal solitons in the Andaman sea (1)

An Atlas of Oceanic Internal Solitary Waves (February 2004)
by Global Ocean Associates
Prepared for Office of Naval Research – Code 322 PO

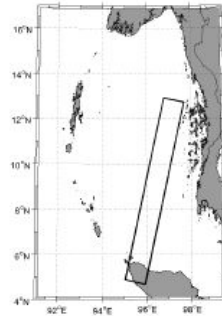
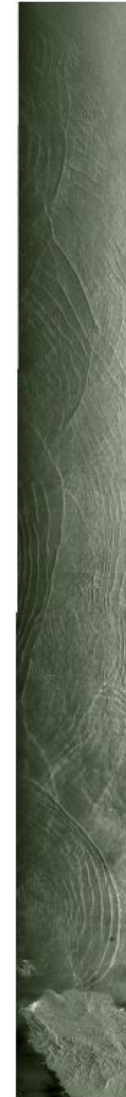
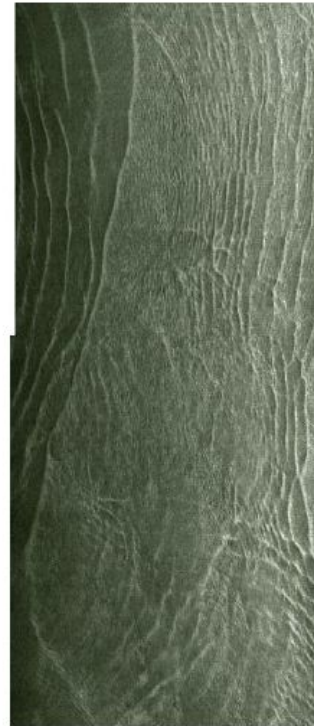


Figure 6. (Right) ERS-2 (C-band, VV) SAR image of the Andaman acquired on 11 February 1997 at 0359 UTC (orbit 9477, frames 3357, 3375, 3393, 3341, 3429, 3447, 3465, 3483, and 3501). The image shows a large number internal wave packets and associated soliton-soliton interaction. Imaged area is 100 km x 900 km. (Below) An enlargement highlighting a middle portion of the image. Imaged area 235 km x 100 km ©ESA 1997.

Andaman Sea



Internal solitons in the Andaman sea (2)

An Atlas of Oceanic Internal Solitary Waves (February 2004)
by Global Ocean Associates
Prepared for Office of Naval Research – Code 322 PO

Andaman Sea

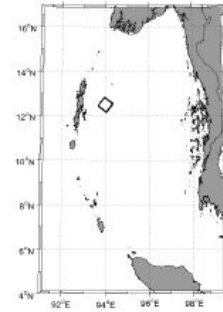
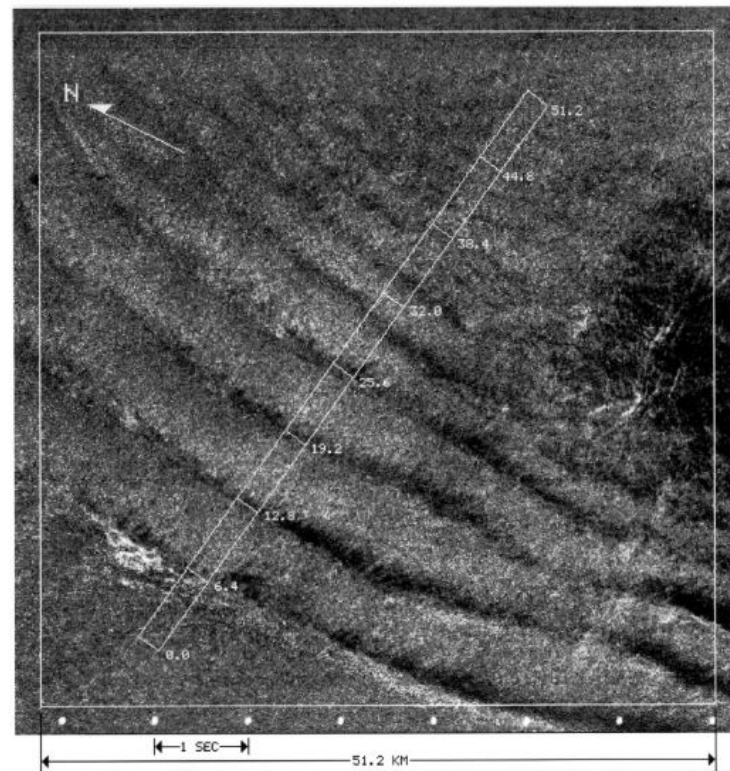
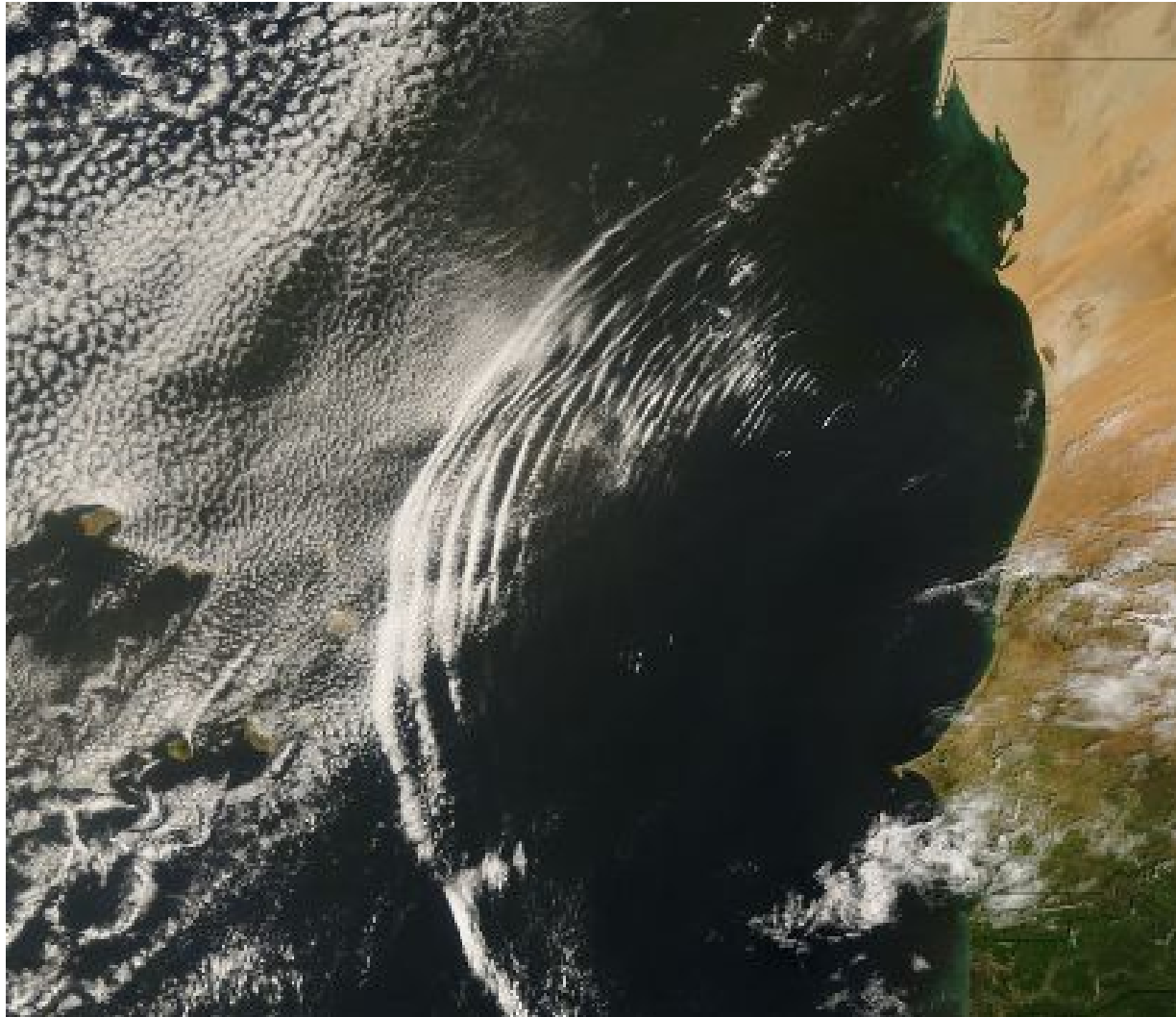


Figure 12. SIR-A (L-band, HH) SAR image near the Andaman Islands acquired on 11 November 1981. The image shows a packet of westward propagating solitons and what is thought to be a rain squall (dark patch at right center). Imaged area is 51.2 km x 51.2 km. [Image courtesy of the Jet Propulsion Laboratory][After Apel et al. 1985]



Solitary clouds west of Africa



Laser plasma experiments on electrostatic waves

PRL 101, 025004 (2008)

PHYSICAL REVIEW LETTERS

week ending
11 JULY 2008

Observation of Collisionless Shocks in Laser-Plasma Experiments

L. Romagnani,^{1,*} S. V. Bulanov,^{2,3} M. Borghesi,¹ P. Audebert,⁴ J. C. Gauthier,⁵ K. Löwenbrück,⁶ A. J. Mackinnon,⁷
P. Patel,⁷ G. Pretzler,⁶ T. Toncian,⁶ and O. Willi⁶

¹*School of Mathematics and Physics, The Queen's University of Belfast, Belfast, Northern Ireland, United Kingdom*

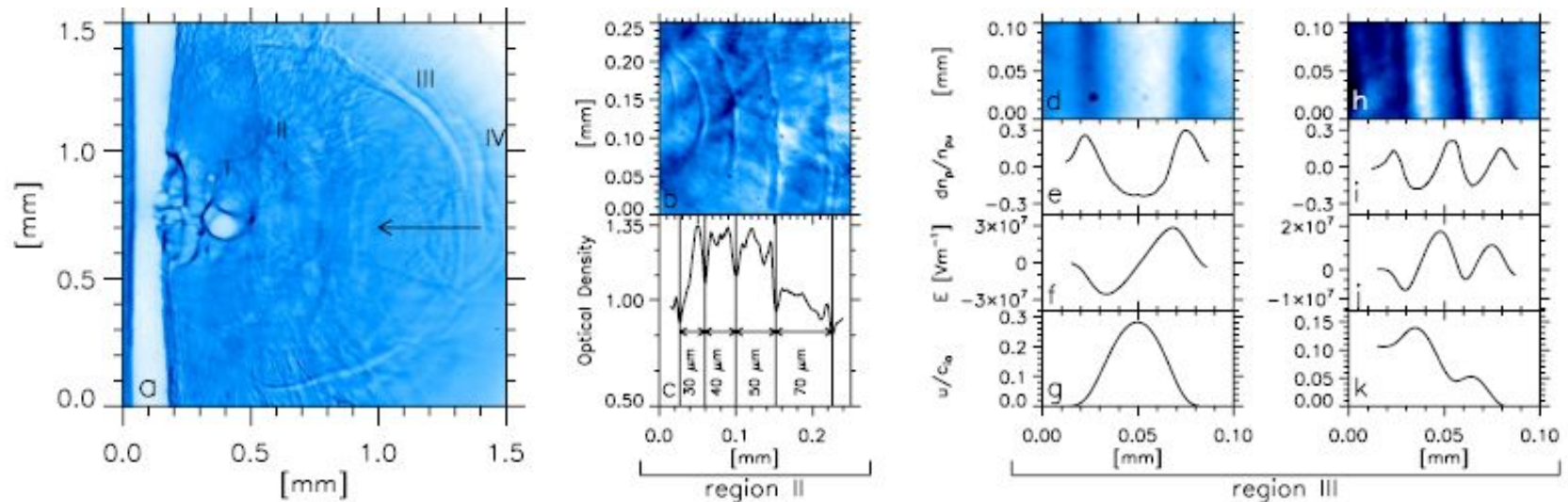


FIG. 1 (color online). (a) Typical proton imaging data taken at the peak of the interaction pulse with protons of 7 MeV energy. Note the strong modulation associated with the ablating plasma in the region I and the modulated pattern ahead of the shock front possibly associated with a reflected ion bunch in the region IV. The arrow indicates the laser beam direction. (b)–(c) Detail and RCF optical density lineout corresponding to the region II showing modulations associated with a train of solitons. (d)–(k) Details of the region III and correspondent lineouts of the probe proton density $\delta n_p/n_{pa}$, reconstructed electric field E , and reconstructed normalized ion velocity u/c_{ia} in the case of an ion acoustic soliton (d)–(g) and of a collisionless shock wave (h)–(k) (the collisionless shock detail corresponds to a different shot not shown here for brevity).

Laser plasma experiments on electrostatic waves (2)

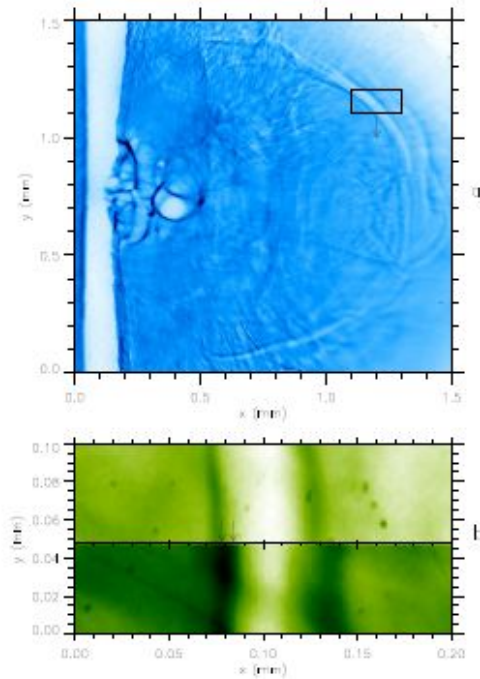


Figure 3.9: a. Proton image showing the ion-acoustic soliton. b Detail of the ion-acoustic soliton at two different times. The relative time between the two frames is ~ 25 ps, and the soliton has moved by $\sim 5 \div 10 \mu\text{m}$.

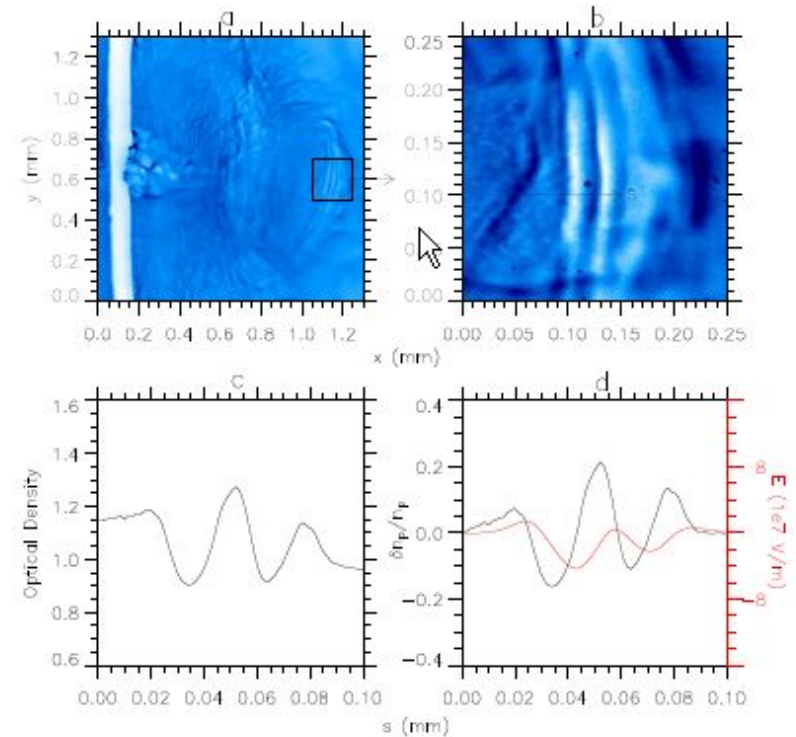


Figure 3.14: a. Proton image taken at the peak of the interaction pulse. b. Detail of the collisionless shock wave. c. Profile of the optical density in the RCF across the collisionless shock. d. Proton density modulation across the shock (black

(courtesy of L Romagnani & M Borghesi, Queen's University Belfast, UK)

Electron-holes observed via proton imaging diagnostics

PHYSICS OF PLASMAS 17, 010701 (2010)

Observation and characterization of laser-driven phase space electron holes

G. Sarri,¹ M. E. Dieckmann,² C. R. D. Brown,³ C. A. Cecchetti,¹ D. J. Hoarty,³ S. F. James,³ R. Jung,⁴ I. Kourakis,¹ H. Schamel,⁵ O. Willi,⁴ and M. Borghesi¹

¹School of Mathematics and Physics, The Queen's University of Belfast, Belfast BT7 1NN, United Kingdom

²ITN, Linköping University, 60174 Norrköping, Sweden

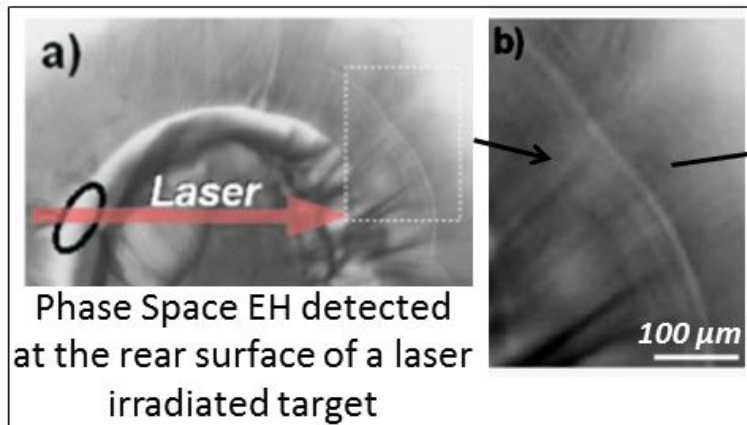
³AWE, Aldermaston, Reading, Berkshire RG7 4PR, United Kingdom

⁴Institute for Laser and Plasma Physics, Heinrich-Heine-University, 40225 Düsseldorf, Germany

⁵Physikalisches Institut, Universität Bayreuth, D-95440 Bayreuth, Germany

(Received 12 November 2009; accepted 15 December 2009; published online 7 January 2010)

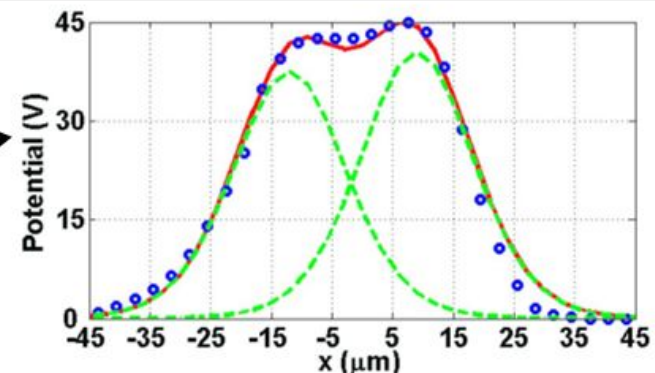
The direct observation and full characterization of a phase space electron hole (EH) generated during laser-matter interaction is presented. This structure, propagating in a tenuous, nonmagnetized plasma, has been detected via proton radiography during the irradiation with a ns laser pulse ($I\lambda^2 \approx 10^{14}$ W/cm²) of a gold *hohlraum*. This technique has allowed the simultaneous detection of propagation velocity, potential, and electron density spatial profile across the EH with fine spatial and temporal resolution allowing a detailed comparison with theoretical and numerical models.



- Incomplete thermalization of the background plasma
- Hot electron population accelerated by the laser



Fit by κ -distributed plasma electron distribution



Potential profile fitted with two bell-shaped, κ -dependent soliton curves:

$$\phi(x) = \phi_{\max} \operatorname{sech}^4 \left(\frac{x}{4\sqrt{\gamma_e}} \right)$$

κ -dependent parameter: $\kappa \sim 4$

Shock creation and particle acceleration driven by plasma expansion into a rarefied medium

G. Sarri,¹ M. E. Dieckmann,² I. Kourakis,¹ and M. Borghesi¹

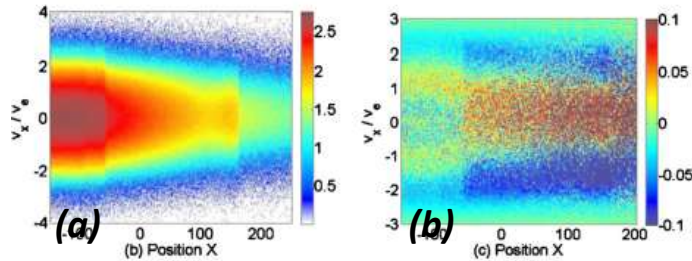
¹Centre for Plasma Physics, The Queen's University of Belfast, Belfast BT7 1NN, United Kingdom

²VITA ITN, Linköping University, 60174 Norrköping, Sweden

(Received 26 March 2010; accepted 6 July 2010; published online 19 August 2010)

The expansion of a dense plasma through a more rarefied ionized medium is a phenomenon of interest in various physics environments ranging from astrophysics to high energy density laser-matter laboratory experiments. Here this situation is modeled via a one-dimensional particle-in-cell simulation; a jump in the plasma density of a factor of 100 is introduced in the middle of an otherwise equally dense electron-proton plasma with an uniform proton and electron temperature of 10 eV and 1 keV, respectively. The diffusion of the dense plasma, through the rarefied one, triggers the onset of different nonlinear phenomena such as a strong ion-acoustic shock wave and a rarefaction wave. Secondary structures are detected, some of which are driven by a drift instability of the rarefaction wave. Efficient proton acceleration occurs ahead of the shock, bringing the maximum proton velocity up to 60 times the initial ion thermal speed. © 2010 American

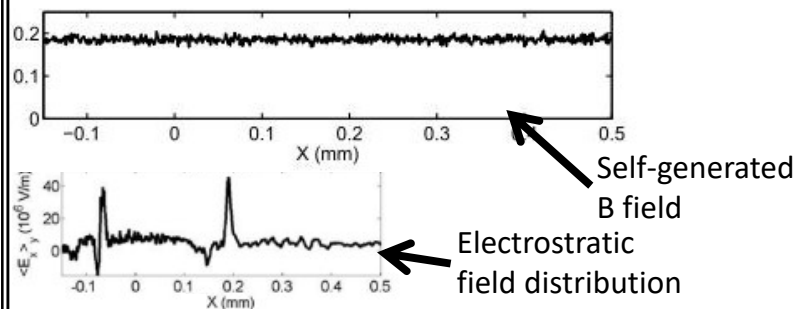
Non-Maxwellian behaviour of the electron density distribution of a plasma expanding into a rarefied medium has been seen in PIC sims



(a) Phase space of the expanding electrons.
(b) Electron distribution function normalised to a Maxwellian with same density and temperature.

Non-thermality generated by the counterstreaming electrons of the rarefied medium.

Suppression of Weibel instability → electrostatic plasma evolution



Clear difference from expansion into vacuum!

ESWs in Space? It all started with the *Northern Lights*...

Aurora

From Wikipedia, the free encyclopedia

Several terms redirect here. For other uses, see [Aurora \(disambiguation\)](#), [Aurora Australis \(disambiguation\)](#), [Aurora Borealis \(disambiguation\)](#), [Northern Lights \(disambiguation\)](#) and [Southern Lights \(disambiguation\)](#).

An **aurora** (plural: **auroras** or **aurorae**),^[a] sometimes referred to as **polar lights** (aurora polaris), **northern lights** (aurora borealis), or **southern lights** (aurora australis), is a natural light display in the Earth's sky, predominantly seen in high-latitude regions (around the Arctic and Antarctic).

Auroras are the result of disturbances in the magnetosphere caused by solar wind. These disturbances are sometimes strong enough to alter the trajectories of charged particles in both solar wind and magnetospheric plasma. These particles, mainly electrons and protons, precipitate into the upper atmosphere (thermosphere/exosphere).

The resulting ionization and excitation of atmospheric constituents emit light of varying color and complexity. The form of the aurora, occurring within bands around both polar regions, is also dependent on the amount of acceleration imparted to the precipitating particles. Precipitating protons generally produce optical emissions as incident hydrogen atoms after gaining electrons from the atmosphere. Proton auroras are usually observed at lower latitudes.^[2]

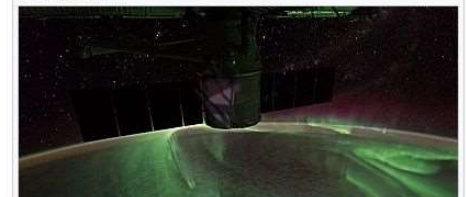
Most of the planets in our solar system, some natural satellites, brown dwarfs, and even comets also host auroras.

Contents [hide]

- 1 Etymology
- 2 Occurrence
 - 2.1 Images
 - 2.2 Forms of auroras
 - 2.3 Colors and wavelengths of auroral light
 - 2.4 Changes with time
 - 2.5 Other auroral radiation
 - 2.6 Aurora noise
 - 2.7 Atypical auroras
 - 2.7.1 STEVE
 - 2.7.2 Picket-fence aurora
- 3 Causes
 - 3.1 Auroral particles
 - 3.2 Auroras and the atmosphere
 - 3.3 Auroras and the ionosphere
- 4 Interaction of the solar wind with Earth
 - 4.1 Magnetosphere
- 5 Auroral particle acceleration
- 6 Auroral events of historical significance
- 7 Historical theories, superstition and mythology
- 8 Non-terrestrial auroras
- 9 See also
- 10 Notes



Images of auroras from around the world, including those with rarer red and blue lights



Double Layers in Space observations – history...

- Mozer et al [PRL 1977] were the first to provide an interpretation of S3-3 satellite data *in the aurora* as double layers (DLs):

Observations of Paired Electrostatic Shocks in the Polar Magnetosphere*

F. S. Mozer, C. W. Carlson, M. K. Hudson, R. B. Torbert, B. Parady, and J. Yatteau
Physics Department and Space Sciences Laboratory, University of California, Berkeley, California 94720

and

M. C. Kelley
School of Electrical Engineering, Cornell University, Ithaca, New York 14854
(Received 6 December 1976)

dc and ac plasma-density and vector-electric-field detectors on a polar orbiting satellite have measured spatially confined regions of extremely large ($\sim \frac{1}{2}$ V/m) electric fields in the auroral zone at altitudes below 8000 km. Such regions frequently have double structures of opposing electric fields containing characteristic and different wave spectra internal and external to themselves. These structures are identified as paired electrostatic shocks which are associated with electrostatic ion cyclotron wave turbulence.

The S3-3 satellite was launched during the summer of 1976 into a nearly polar orbit with perigee and apogee altitudes of 260 and 8050 km, respectively. On-board instruments have made the first *in situ* measurements of dc electric fields at auroral latitudes and altitudes where particle-acceleration, kilometric-radiation-generation,

measured potential differences yield three orthogonal components of the static or fluctuating electric field. Four of the spheres are located at the ends of four 18-m wire booms that are maintained in the satellite spin plane by centrifugal force. The remaining pair of spheres are oriented along the vehicle spin axis on 3-m rigid

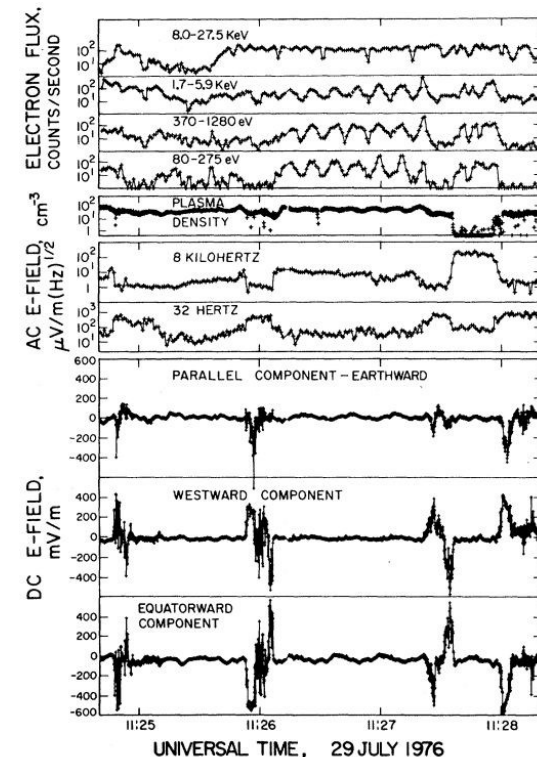


FIG. 1. Field and particle measurements made on a satellite during its poleward-bound passage through extremely large dc-electric-field regions in the northern auroral zone. The particle data are modulated at twice the satellite spin frequency.

DLs vs Electrostatic Shocks & Solitary Waves

- Inspired by Mozer et al [PRL 1977], Witt and Lotko [Phys. Fluids, 1978] modelled pulse-shaped observations as *paired* ion-acoustic shocks:

Ion-acoustic solitary waves in a magnetized plasma with arbitrary electron equation of state

E. Witt and W. Lotko

Space Sciences Laboratory, University of California, Berkeley, California 94720

(Received 17 August 1982; accepted 6 April 1983)

The oblique propagation of fully nonlinear, slow ion-acoustic solitary waves in a collisionless, low-beta, magnetized plasma is examined. The analysis includes the effects of a finite ion pressure, electron trapping, and multicomponent particle populations. The existence of both compressive and rarefactive modes propagating obliquely to the magnetic field in a plasma with two distinct Boltzmann electron populations and cold ions is demonstrated. It is shown that paired electrostatic shocks observed over the Earth's auroral zone may be closely related to the rarefactive modes. As a measure of the collisionless dissipation encountered by the solitary waves, the linear response of the plasma to slow ion-acoustic waves is also examined.

I. INTRODUCTION

Ion-acoustic solitary waves have been observed in laboratory plasmas, and much progress has been made in theory. Unmagnetized versions of these waves have been extensively studied. (See Tran¹ for a review.) It is also of interest to determine how a magnetic field affects the propagation of these waves. One motivation comes from the field of space physics. Recent electric field measurements^{2,3} in space indicate that localized nonlinear plasma waves generally accompany and are possibly responsible for the acceleration of auroral particles to kilovolt energies. The observed waves, referred to as paired electrostatic shocks, propagate at speeds much less than the electron thermal speed, suggesting that they may be related to nonlinear electrostatic waves propagating as slow or intermediate modes.⁴ Numerical studies⁵⁻⁷ of

In this paper we present the first finite-amplitude, magnetized analysis of nonlinear ion-acoustic waves in which $N_e(\Psi)$ is arbitrary and in which the ions may have a finite temperature. As in previous treatments, the nonlinear plasma response is described by time stationary fluid equations for the relatively cold ions and by Poisson's equation in the quasineutral approximation. The quasineutral approximation allows us to study only waves with finite angles of propagation relative to the uniform magnetic field, and the approximation requires the solutions to have "slowly changing" electric fields. This is discussed in more detail in Sec. II. Our treatment, for arbitrary $N_e(\Psi)$, allows us to make general statements about the resulting nonlinear wave solutions. For instance, previous authors have found, using the Boltzmann electron approximation, that waves can exist only when their speed v_p lies in the range $c_s \cos \theta < v_p < c_s$, where θ is the angle of propagation relative to the magnetic

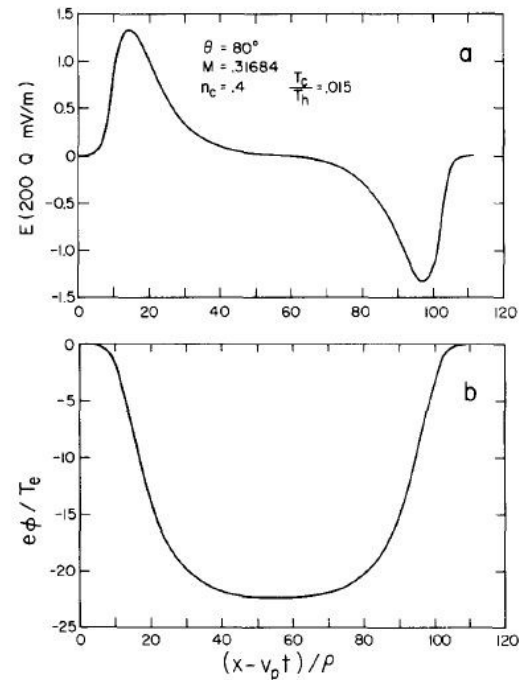


FIG. 7. Numerical solitary wave solution of Eq. (17) for a two-temperature Boltzmann electron and cold ion plasma model. The wave is rarefactive and propagates at $\theta = 80^\circ$ relative to the magnetic field. Other parameters of the solution are indicated in the figure. (a) Electric field in units of $200 Q$ mV/m where $Q = (f_{ei}/100 \text{ Hz})(T_e/10 \text{ eV})^{1/2}$. For example, when $f_{ei} = 100 \text{ Hz}$ and $T_e = 10 \text{ eV}$, the peak electric field is about 280 mV/m . (b) Normalized electric potential profile.

Electrostatic Solitary Waves (ESWs) – history...

- ESWs –to be distinguished from DLs–were first observed in the auroral region in 1982 [Temerin et al, PRL 1982], using satellite S3-3 data...

VOLUME 48, NUMBER 17

PHYSICAL REVIEW LETTERS

26 APRIL 1982

Observations of Double Layers and Solitary Waves in the Auroral Plasma

M. Temerin, K. Cerny, W. Lotko, and F. S. Mozer

Space Sciences Laboratory, University of California, Berkeley, California 94720

(Received 29 January 1982)

Small-amplitude double layers and solitary waves containing magnetic-field-aligned electric field components have been observed for the first time in the auroral plasma between altitudes of 6000 and 8000 km in association with electron and ion velocity distributions that indicate the presence of electric fields parallel to the magnetic field. The double layers may account for a large portion of the parallel potential drop that accelerates auroral particles.

PACS numbers: 53.35.Fp, 52.35.Mw, 94.30.Gm

Double layers, small localized regions of a single electric field polarity, have been studied analytically,¹ but until now have been observed only in computer simulations² and in laboratory plasmas.³ We report the first observation of small-amplitude double layers in a naturally occurring plasma. These double layers differ from the previously reported electrostatic shocks⁴

in that their electric field is much smaller (typically no greater than 15 mV/m), their electrostatic polarization relative to the magnetic field is predominantly parallel rather than perpendicular, and the duration of an individual double layer is much shorter—typically 2–20 ms rather than 0.1–10 s for the electrostatic shocks. The dominant polarity of the electric field through an

ESWs: a common occurrence in Space plasma observations

- ESWs occur in abundance as magnetic-field aligned *bipolar* electric field structures (among other forms), observed in abundance in satellite data (Cluster, FAST, ...)
- Solitary waves: potential pulses, solitons, double layers, flat-topped pulses, ...

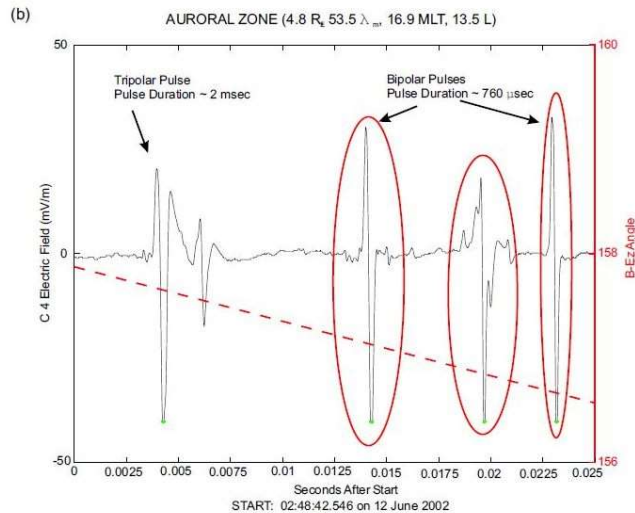


Fig. 1. Cluster WBD data taken on 12 June 2002 in the auroral zone. (a) Spectrogram showing the frequency and power spectral density of the emissions. The broad-band signals ranging up to about 10 kHz are indicative of times when IES are observed. (b) Representative waveform from a time of the broad-band signals, showing the two types of IES: bipolar and tripolar pulses.

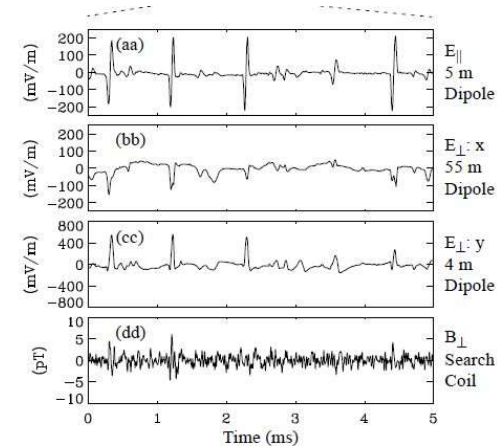


Figure 5. (From [5]) (a) The electric field parallel to B_0 . (b) The electric field perpendicular to B_0 (ΔE_{\perp}) and in the spin plane of the satellite. This signal, measured by a 56 m dipole antenna, appears attenuated, indicating that the structure size may have been < 112 m. (c) ΔE_{\perp} along the spin axis of the satellite. (d) A perturbation magnetic field perpendicular to B_0 (ΔB_{\perp}). ΔB_{\perp} was filtered to a pass band (3 kHz–16 kHz) to expose the weak signals and therefore may not appear unipolar in this figure. (aa)–(dd) An expanded view of this data.

Figures from: Pickett *et al* Ann. Geophys. (2004) (L, Cluster), Ergun *et al*, PPCF (1999) (R, FAST)

ESWs near Saturn (Enceladus) - Cassini mission

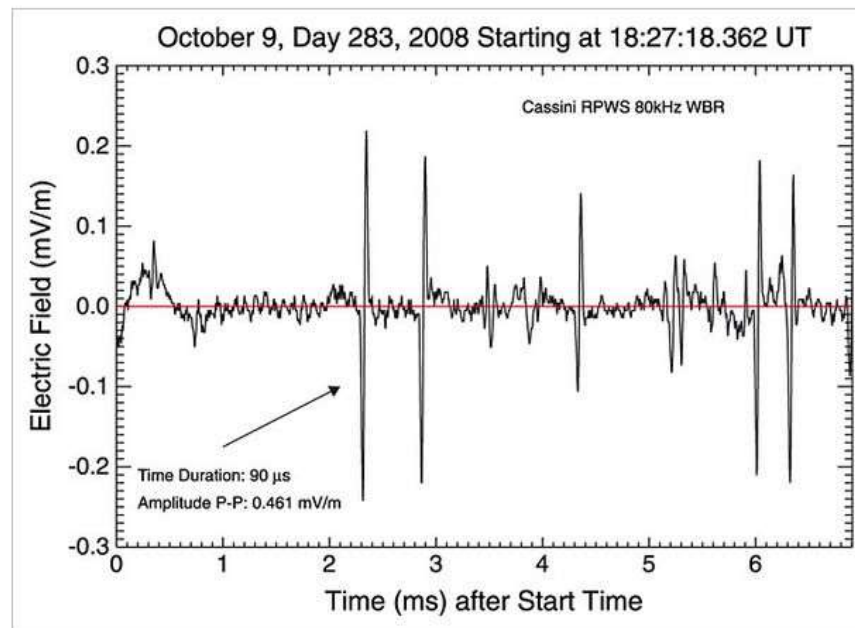


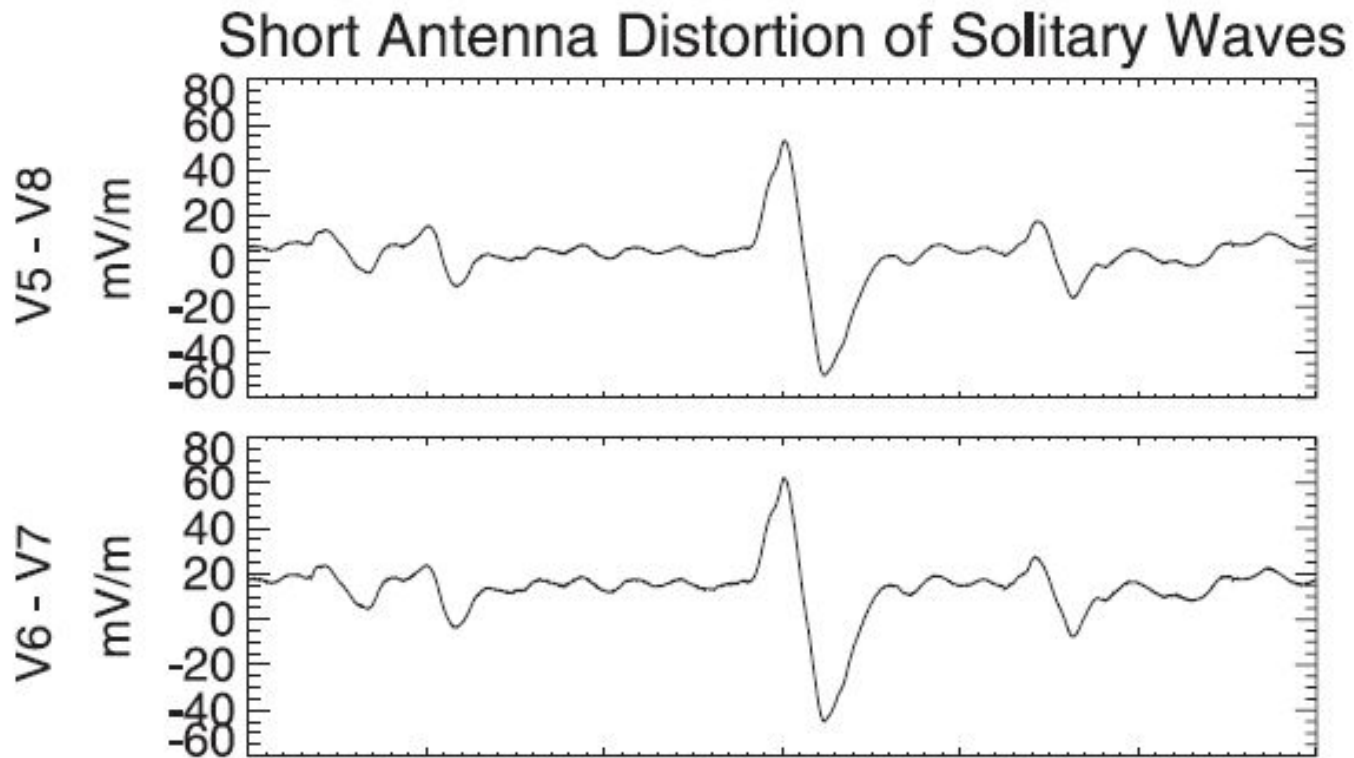
Figure 2

[Open in figure viewer](#) | [PowerPoint](#)

Time series data of the calibrated electric field data over a ≈ 7 ms interval from the Cassini RPWS WBR, 80 kHz filter bandwidth, obtained on 9 October 2008, ~ 0.5 h before crossing the Enceladus dust plume. These data show five well-defined bipolar ESW pulses embedded within a much lower amplitude oscillatory wave. Note that the amplitudes of these ESWs are comparable to those in Figure 1, but their time durations are much shorter.

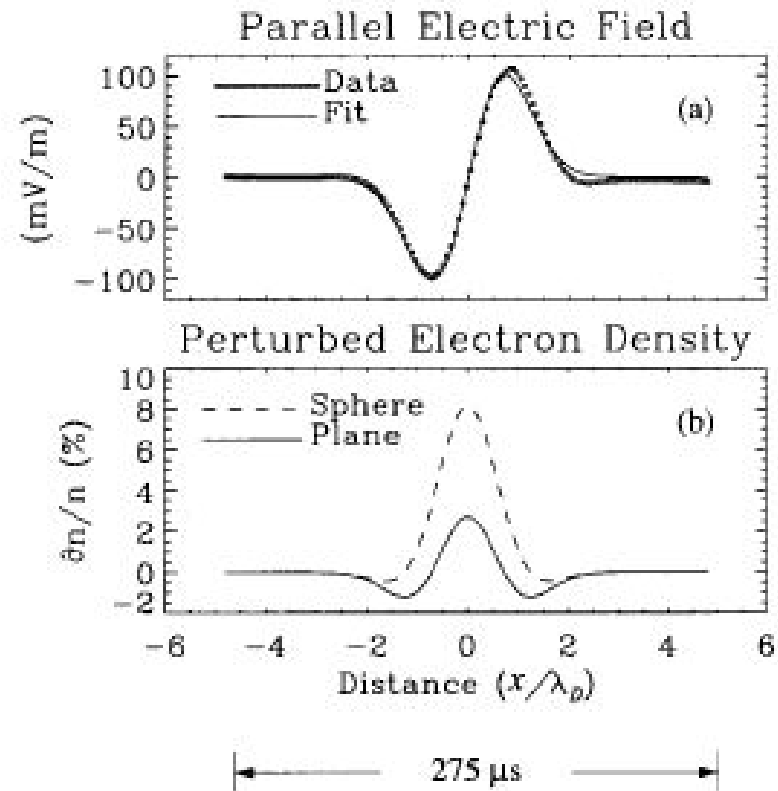
Source: JS Pickett et al, JGR Space Physics **120** (8), 6569 (2015)

FAST satellite observations of large solitary spikes in the Earth's *auroral* region



FAST auroral observations (2)

Ergun, et al.: Properties of fast solitary structures



Nonlinear Processes in Geophysics (1999) 6: 187–194

Properties of fast solitary structures

R. E. Ergun, C. W. Carlson, L. Muschietti, I. Roth, and J. P. McFadden

Space Sciences Laboratory, University of California, Berkeley, CA, 94720, USA

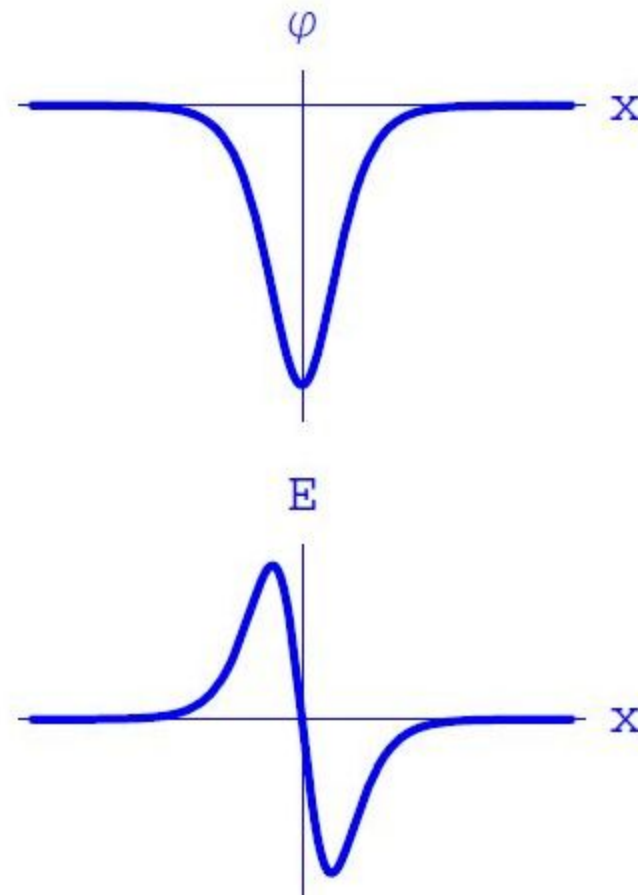
Received: 15 June 1999 – Revised: 6 September 1999 – Accepted: 13 September 1999

Abstract. We present detailed observations of electromagnetic waves and particle distributions from the Fast Auroral SnapshoT (FAST) satellite which reveal many important properties of large-amplitude, spatially-coherent plasma structures known as “fast solitary structures” or “electron phase space holes”. Similar structures have been observed in

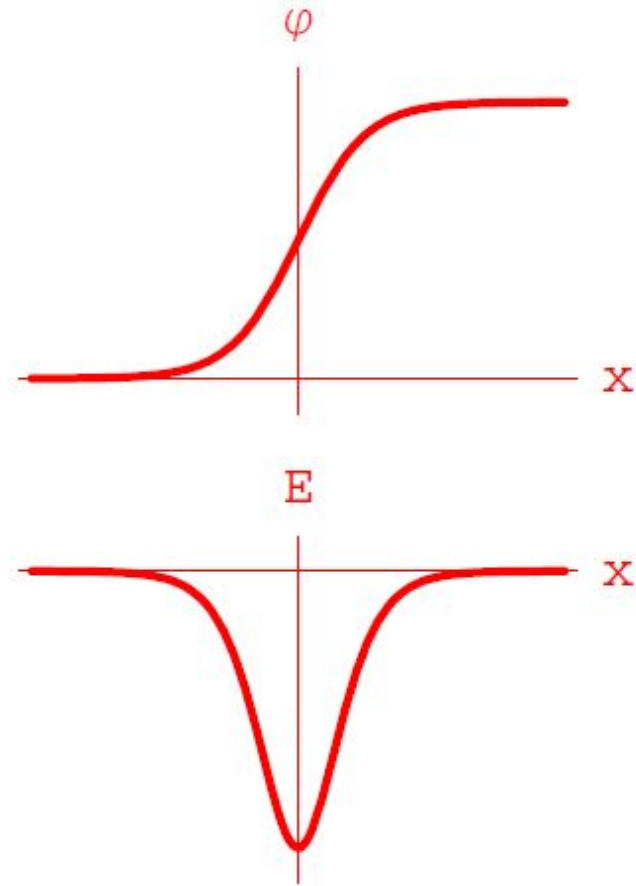
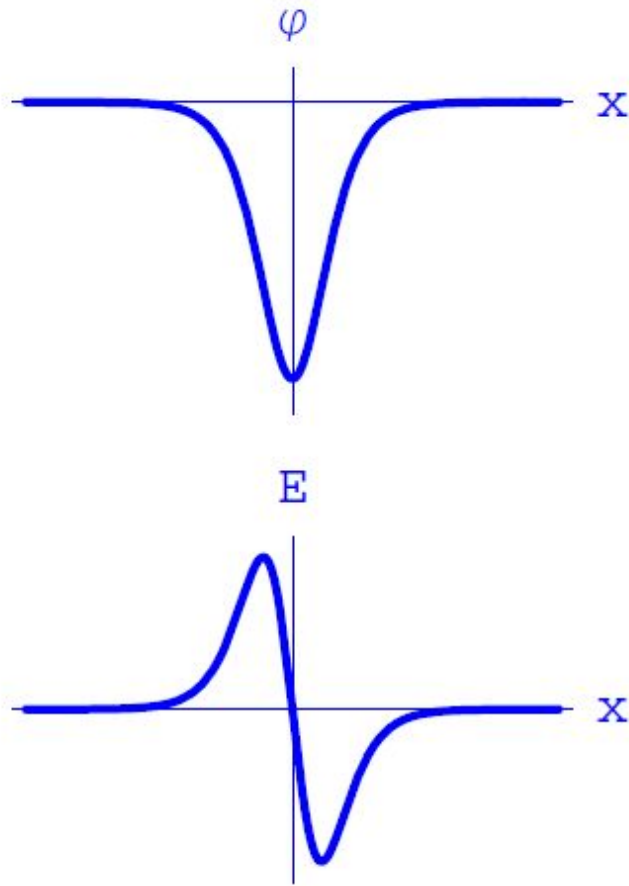
which distinguish acoustic solitons (Ergun et al., 1982). The structure is brief, electrostatic and that FAST has

Fig. 5. (From Ergun et al., 1998c) (a) ΔE_{\parallel} . The dots are the data at 0.5 μ s resolution translated into Debye lengths assuming a constant parallel velocity, $v_{sol} = 3.2 \times 10^6$ m/s. The smooth trace is the fit to Eq. (2). (b) Calculated charge densities assuming spherical and planar geometry. The plasma conditions were $n_e = 5.7 \pm 2.0$ cm⁻³, $T_{e\parallel} = 704 \pm 145$ eV, $v_{sol} = 3.2 \times 10^6 \pm 1.1 \times 10^6$ m/s, $T_{i\perp} = 370 \pm 74$ eV, $|B_0| = 11481 \pm 10$ nT, $\lambda_D = 82 \pm 30$ m, and $\rho_{H^+} = 241 \pm 24$ m.

Electrostatic potential and electric field bipolar structures (1)



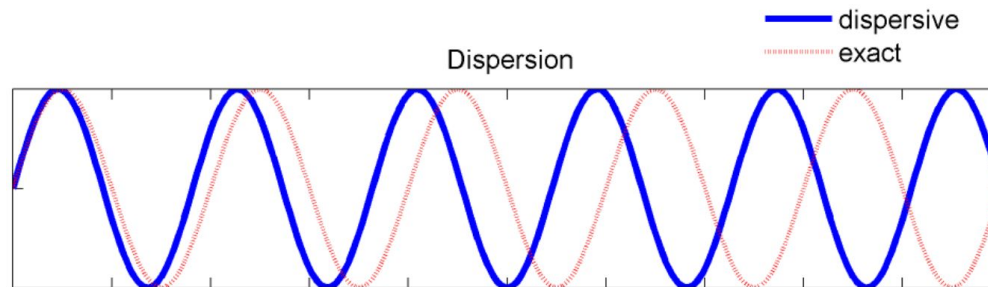
ES potential and E-field: *bipolar* vs *monopolar* structures (2)



Solitary waves require a balance between:

– **Dispersion**, manifested via:

- wave spreading in Fourier space: different modes (\mathbf{k}) travel at different speeds:

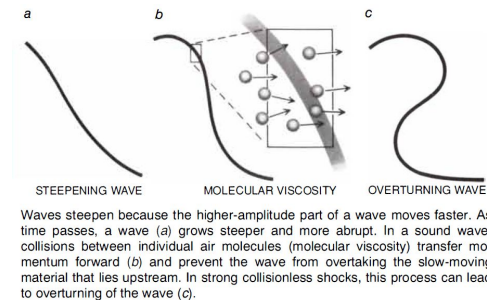


(Source: <http://www.scholarpedia.org>)

- Chromatic dispersion effect in Optics (*rainbow!*)
- Curvature in the dispersion curve $\omega = \omega(k)$, in solid state physics.
- The phase speed $v_{ph} = \frac{\omega}{k} = f(\mathbf{k})$ is a function of the wavenumber \mathbf{k} .

... and **Nonlinearity**, manifested as:

- Amplitude-dependence of the phase speed: larger amplitudes travel faster!
- This results in wave steepening, and eventually wave-breaking:



... a physical phenomenon well-known to seafarers (or *surfers*):



Further traces of nonlinearity include:

- *Secondary harmonic generation.*
- *No superposition principle:* different normal (Fourier) modes do not sum up.
- *Sidebands* appear in the Fourier spectrum.
- ***Energy localization*** (to be discussed later).

Korteweg de Vries (KdV) theory for electrostatic waves

Taniuti and Wei [J. Phys. Soc. Jpn. **24**, 941 (1968)] propose their *reductive perturbation technique*, for long-wavelength ES *acoustic modes* in plasmas.

We review the basic qualitative aspects of this technique below.

- Dispersion relation (*acoustic mode*):

$$\omega \simeq v_{ph}k + Ak^3 + \dots ,$$

(where A is to be determined, for a given plasma composition), thus

$$kx - \omega t \simeq k(x - v_{ph}t) - Ak^3t + \dots$$

- Appropriate space/time stretching

$$\xi = \epsilon^{1/2}(x - Vt), \quad \tau = \epsilon^{3/2}t \quad (V \in \mathfrak{R})$$

- $n \simeq n_0 + \epsilon n_1 + \epsilon^2 n_2 + \dots$; $u \simeq \epsilon u_1 + \epsilon^2 u_2 + \dots$; $\phi \simeq \epsilon \phi_1 + \epsilon \phi_2 + \dots$

Plasma fluid *toy-model* for electrostatic waves (1D)

Continuity (for plasma species s , e.g. *ions*):

$$\frac{\partial n_s}{\partial t} + \frac{\partial \phi}{\partial x} (n_s u_s) = 0$$

Mean velocity u_s equation:

$$\frac{\partial u_s}{\partial t} + u_s \frac{\partial u_s}{\partial x} = -\frac{q_s}{m_s} \frac{\partial \phi}{\partial x}$$

The potential Φ obeys *Poisson's eq.*:

$$\frac{\partial^2 \phi}{\partial x^2} = -4\pi \sum_s q_s n_s = 4\pi e (n_e - Z_i n_i + \dots)$$

- At a given dynamical scale for species s ($= e, i, d$, i.e. electrons, ions, dust, ...), the state of other species may be prescribed by simplifying assumptions;
- Typical paradigm: for ion-acoustic waves ($s = i$), *ions* are inertial, so *electrons* are assumed at equilibrium (e.g. Maxwellian: $n_e \sim e^{e\phi/k_B T_e}$).

- The method is rather tedious yet straightforward; details are omitted here.
- *Korteweg-de Vries (KdV) equation:*

$$\frac{\partial \psi}{\partial \tau} + A \psi \frac{\partial \psi}{\partial \xi} + B \frac{\partial^3 \psi}{\partial \xi^3} = 0.$$

- ★ $\psi = \phi_1$ denotes a small ($\sim \epsilon \ll 1$) correction to the electric potential,
- ★ Constraint: $V = c_s \rightarrow$ propagation at (or slightly above) the sound speed.
- ★ The coefficients A and B incorporate the physics of the particular problem considered, as they contain the dependence on relevant plasma parameters (lengthy expressions omitted here).
- ★ The *dispersion coefficient* B is positive;
- ★ The *nonlinearity coefficient* A determines the soliton polarity, i.e., the sign (positive/negative) of the soliton pulse (\rightarrow *next slide*).

- The soliton solution of the KdV equation above reads:

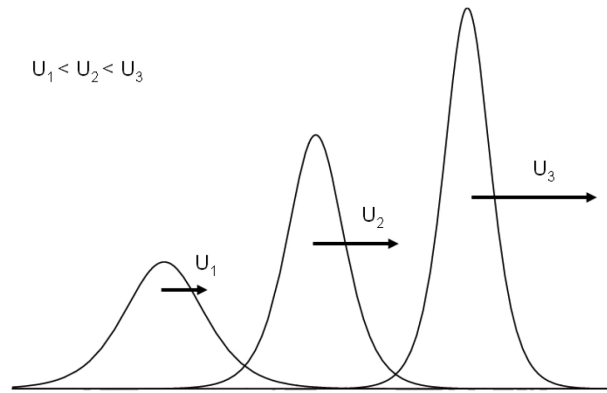
$$\psi = \psi_0 \operatorname{sech}^2 \left(\frac{\xi - U\tau}{L} \right)$$

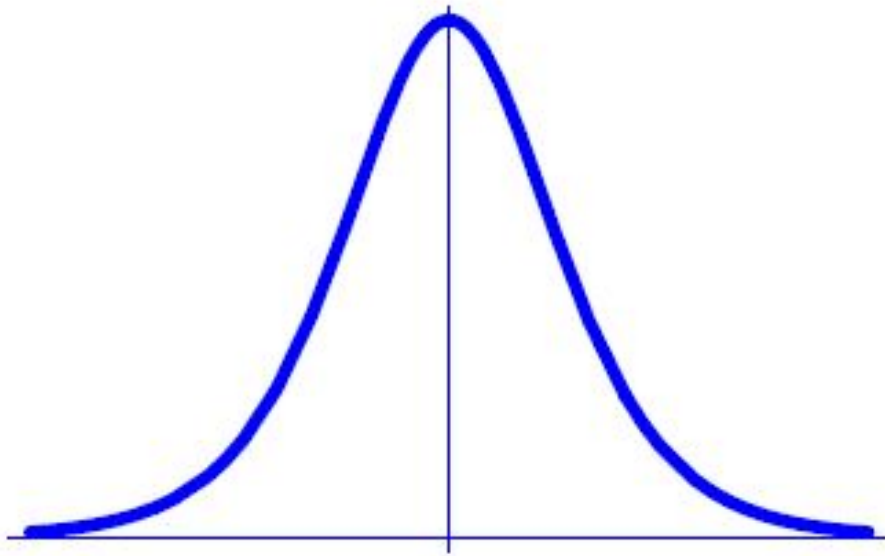
which represents a propagating pulse.

Here:

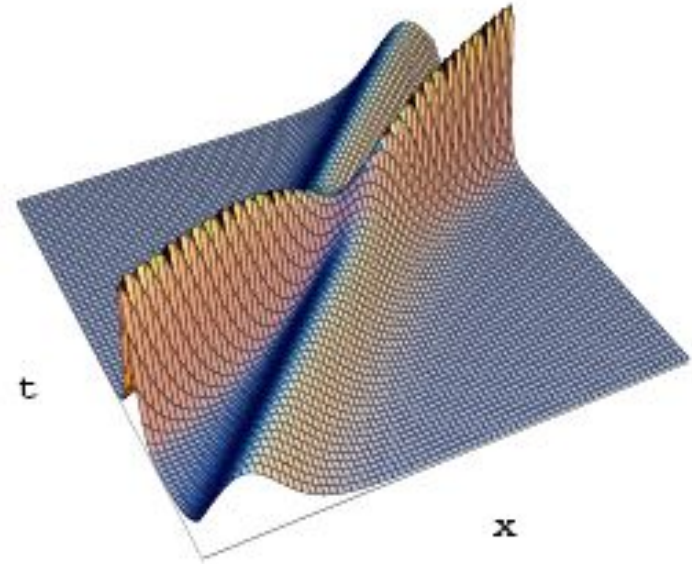
- ★ U is the soliton velocity increment (total soliton speed = $c_s + \epsilon U$)
 - ★ $\psi_0 = \frac{3U}{A}$ is the maximum *soliton amplitude*, and
 - ★ $L = 2\sqrt{B/U}$ is the *soliton width*.
- **Width-amplitude relation:** $\psi_0 L^2 = 12B/A = \text{constant}$, thus *faster* solitons

are *taller* and *narrower*:



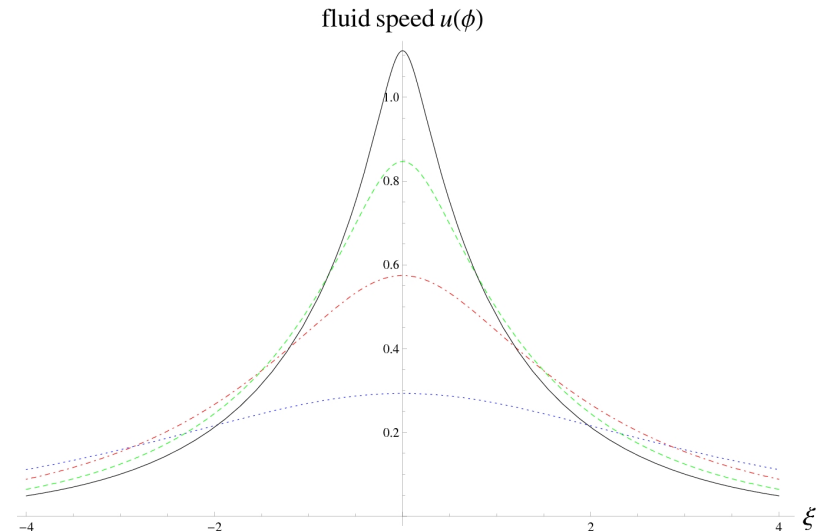
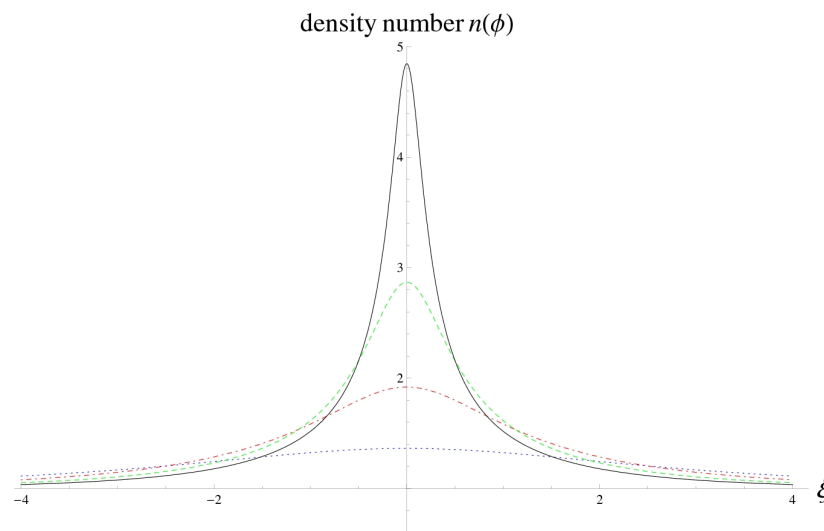
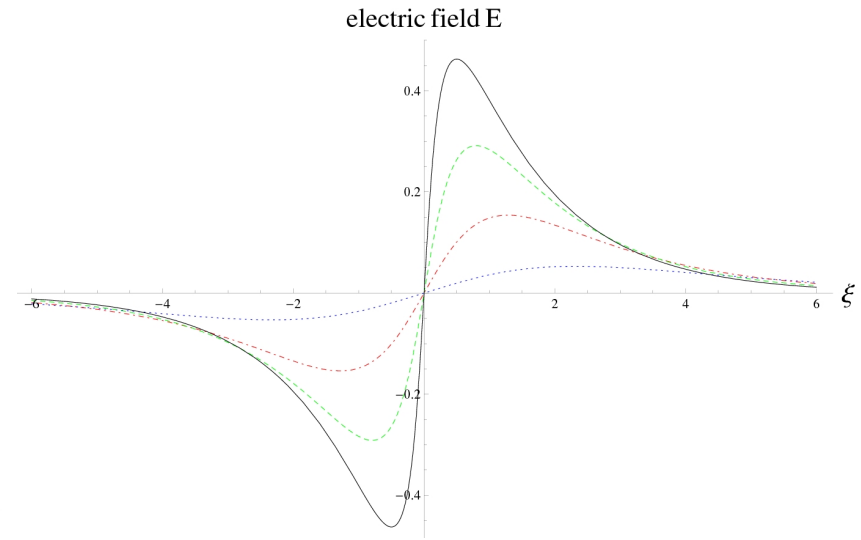
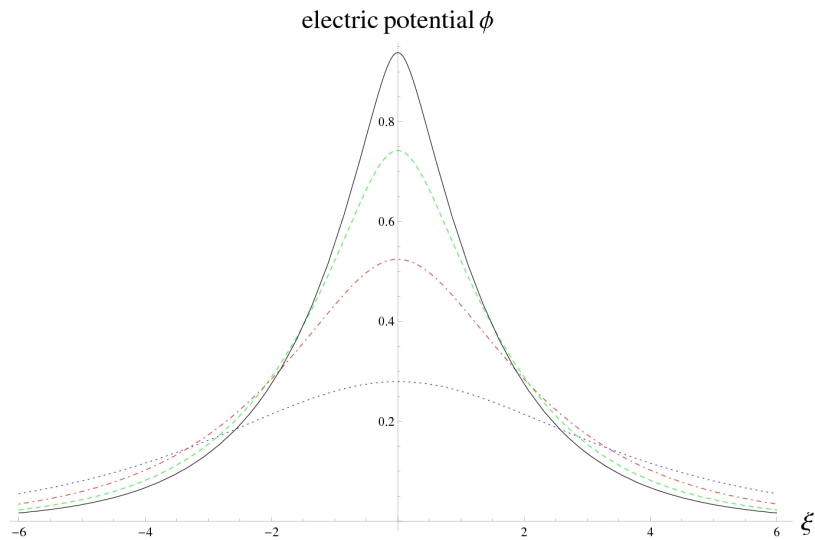


*Typical shape of positive potential
KdV soliton (in arbitrary units)*



*Typical interaction between two
positive potential KdV solitons*

Solution in terms of ϕ + ambipolar field $E = -\nabla\phi$ and fluid variables n, u



Mind the gap...

Restricted validity: The KdV theory obeys certain constraints & limitations

- It is a *small-amplitude* theory: not suitable for strong excitations (off equilibrium);
- Solutions are *weakly* super-acoustic;
- The methodology only works for *acoustic*-type modes (frequency = zero for infinite wavelength); optical modes (or e.g. Langmuir waves in plasmas) are not covered!

Electrostatic solitary waves

A “toy-model”: cold ion fluid + kappa-distributed electrons

Continuity:
$$\frac{\partial n}{\partial t} + \frac{\partial(nu)}{\partial x} = 0$$

Momentum:
$$\frac{\partial u}{\partial t} + u \frac{\partial u}{\partial x} = - \frac{\partial \phi}{\partial x}$$

Poisson Eq.:
$$\frac{\partial^2 \phi}{\partial x^2} = -n + n_e$$

S/thermal electrons:
$$n_e = n_{e,0} \left(1 - \frac{\phi}{\kappa - 3/2}\right)^{-\kappa + 1/2}$$

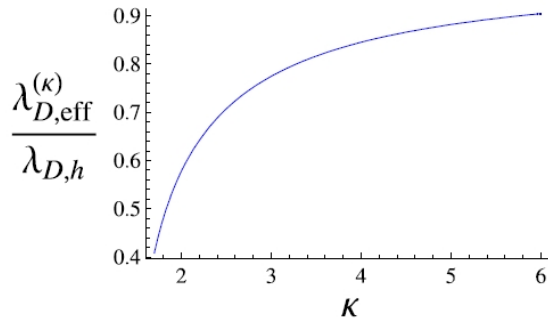
Scaling:
$$n = \frac{n_i}{n_{i0}}, \quad u = \frac{u_i}{c_s}, \quad x = \frac{x}{\lambda_D}, \quad \phi = \frac{e\phi}{k_B T_e}, \quad t = \omega_{pi} t$$

$$c_s = \left(\frac{k_B T_e}{m_i}\right)^{1/2}, \quad \omega_{pi} = \left(\frac{4\pi n_{i0} e^2}{m_i}\right)^{1/2}, \quad \lambda_D = \left(\frac{k_B T_e}{4\pi n_{i0} e^2}\right)^{1/2}$$

[Work in collaboration with: NS Saini, S Sultana, T Baluku, M Hellberg]

Linear regime: modified linear dispersion relation

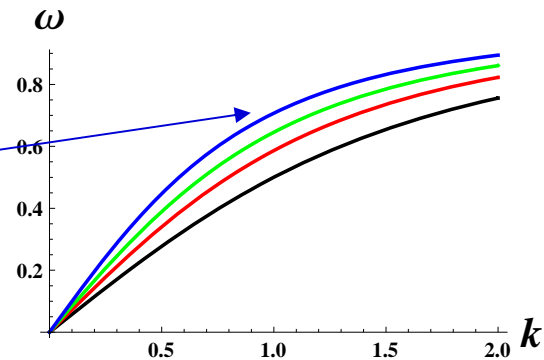
$$\omega^2 = \frac{k^2}{k^2 + c_1} \rightarrow c_1 = \frac{2\kappa - 1}{2\kappa - 3}$$



*κ-modified Debye screening:
Shorter Debye length for small κ!*

Figure 1. Variation of the electrostatic screening (effective Debye) length (scaled) with the superthermality parameter κ . See that the curve approaches unity at the infinite κ limit.

Blue: $\kappa = \infty$ (Maxwellian)
Green: $\kappa = 4$
Red: $\kappa = 2.6$
Black: $\kappa = 2$



(*) [Agreement with Bryant JPP (1996), Mace & Hellberg (PoP 1995)]

Pseudopotential formalism for ion-acoustic travelling waves

[Vedenov & Sagdeev 1961, Sagdeev 1966, Verheest & Hellberg 2009 (review)]

- stationary frame, single travelling coordinate $\xi = x - Mt$
- * reduction of the fluid model PDEs in $\{x, t\}$ to an ODE in ξ
- * **pseudo-energy-balance equation** (for *e-i plasma*):

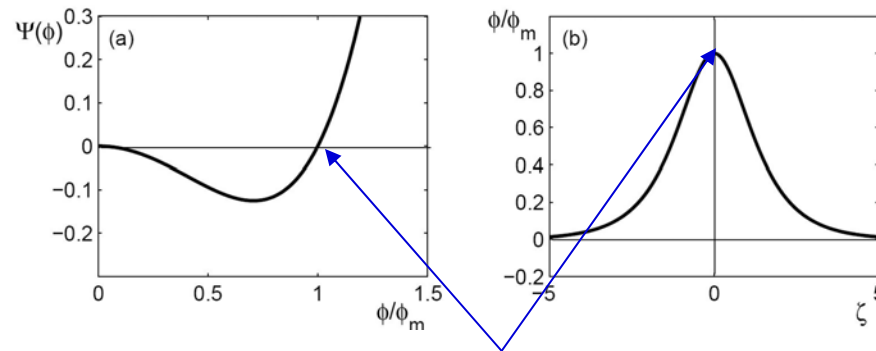
$$\frac{1}{2} \left(\frac{d\phi}{d\xi} \right)^2 + V(\phi) = 0$$

$$V(\phi) = M^2 \left(1 - \sqrt{1 - \frac{2\phi}{M^2}} \right) + 1 - \left(1 - \frac{\phi}{\kappa - 3/2} \right)^{-\kappa + 3/2}$$

- * solution obtained (numerically) for the electric potential ϕ
- * density and fluid velocity given by

$$n = \frac{1}{\sqrt{1 - 2\phi/V^2}} \quad v = V - \sqrt{V^2 - 2\phi}$$

The generic solitary wave (pulse) solution bears the form:

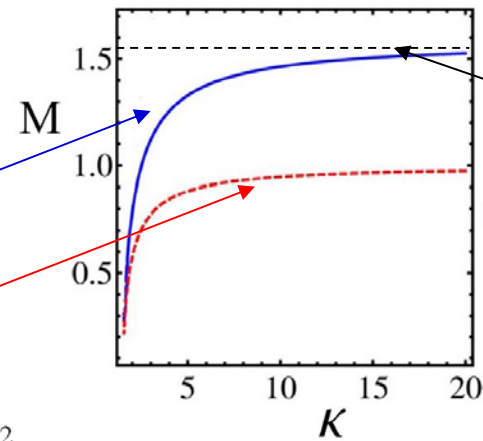


potential pulse amplitude = root of V

Slower “supersonic” (but no subsonic!) solitons
for smaller kappa values:

M_2 : infinite compression point
(choked flow)

M_1 : κ -dependent “sound speed” $M_1 \equiv \left(\frac{\kappa - 3/2}{\kappa - 1/2} \right)^{1/2}$



Known asymptotic limit 1.58
for infinite κ
i.e. for Maxwellian electrons

FIG. 1. (Color online) IA soliton existence domain in the parameter space of κ and Mach number, M . Solitons may be supported in the region between the two curves. The lower, dashed curve represents the minimum (soliton) condition, M_1 , and the upper, solid curve the infinite compression limit, M_2 .

Ion-Acoustic Super Solitary Waves in Dusty Multispecies Plasmas

Alexander E. Dubinov and Dmitry Yu. Kolotkov

Abstract—The concept of a new form of solitary waves—super solitary waves—is proposed, specific for embracing one or several interior separatrices on their wave phase portraits. The super solitary waves of an ion-acoustic type exist, for example, in non-magnetized plasma containing five species of charged particles. For such plasma, electrostatic potential for ion-acoustic super solitary waves is calculated. The super solitary waves can be easily identified among usual solitons, e.g., in differential circuits installed into the measuring channel.

Manuscript received November 20, 2011; revised February 7, 2012; accepted February 20, 2012. Date of publication April 6, 2012; date of current version May 9, 2012. This work was supported in part by a grant of the foundation “Dynasty” and in part by Grant RFBR# 10-02-90418-Ukr_a.

A. E. Dubinov is with the Russian Federal Nuclear Center—All-Russian Scientific and Research Institute of Experimental Physics (RFNC-VNIIEF), 607188 Sarov, Russia, and also with Sarov Institute of Physics and Technology (SarFTI), National Research Nuclear University “MEPhI,” 607188 Sarov, Russia (e-mail: dubinov@ntc.vniief.ru).

D. Y. Kolotkov is with Sarov Institute of Physics and Technology (SarFTI), National Research Nuclear University “MEPhI,” 607188 Sarov, Russia (e-mail: molotok300@gmail.com).

Digital Object Identifier 10.1109/TPS.2012.2189026

separatrices and a number of equilibrium points. Then, there is a new form of a solitary wave, never described before—a super solitary wave corresponding to the exterior separatrix.

Can super solitary waves exist in plasma? In this paper, it is proven that super solitary wave can exist, for instance, in the case of ion-acoustic waves in dusty multispecies plasmas containing electrons, positrons, and two types of ions of the different signs of charge and dust particles. Notably, various

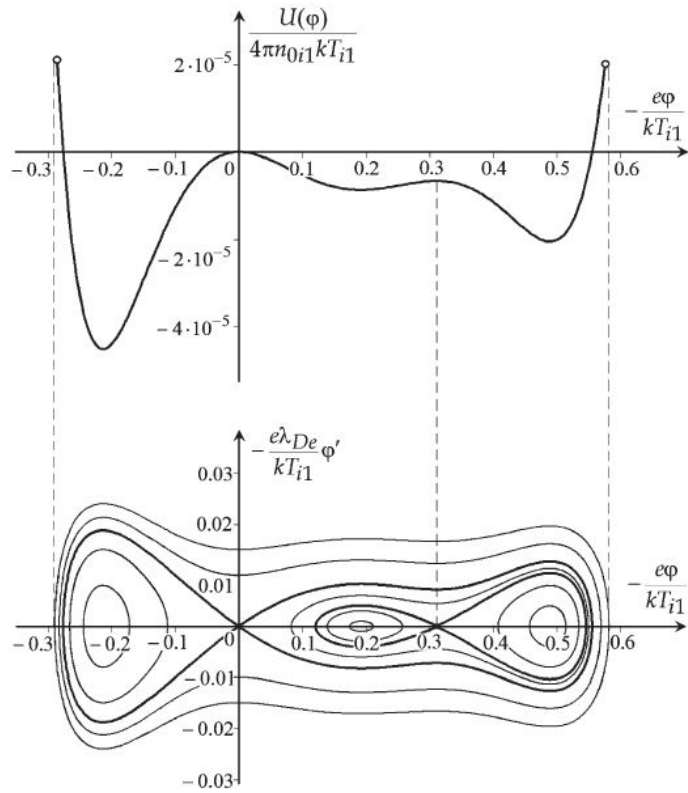


Fig. 2. Plot of pseudopotential (the upper end points, corresponding to the reflection of ions from the potential barrier in the wave, are shown by circles) and the phase wave portrait (in the lower part, separatrices are shown by heavy line). λ_{De} is the electron Debye length.

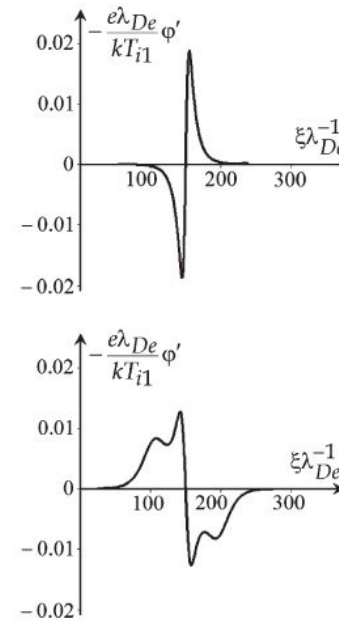


Fig. 4. Profile of the derivatives of (top) a normal soliton and (bottom) a super solitary wave.

Super solitary waves exist in plasma consisting **no fewer than four charged species** of particles (in our case, there are five species). In simpler two- or three-species plasmas, the Sagdeev pseudopotential has no more than one or two minima, and the case when one separatrix is embraced by another external separatrix is not possible; so, super solitary waves do not exist with such a set of parameters.

GENERAL ASPECTS
OF HIGH ENERGY CHEMISTRY

Interpretation of Ion–Acoustic Solitons of Unusual Form
in Experiments in SF₆–Ar Plasma

A. E. Dubinov and D. Yu. Kolotkov

Sarov Physicotechnical Institute, Branch of “Moscow Engineering Physics Institute” National Nuclear Research University,
ul. Dukhova 6, Sarov, Nizhni Novgorod oblast, 607188 Russia
e-mail: dubinov-ae@yandex.ru

Received May 2, 2012; in final form, May 23, 2012

Abstract—The emergence in SF₆–Ar plasma of ion–acoustic solitons with angular profiles or profiles with several maxima has been explained. It has been shown that the cause of these profiles is that the phase trajectories of the solitons of this type in the phase portrait cover one or more separatrices, which in turn can appear only in plasma with a complex chemical composition.

DOI: 10.1134/S0018143912060033

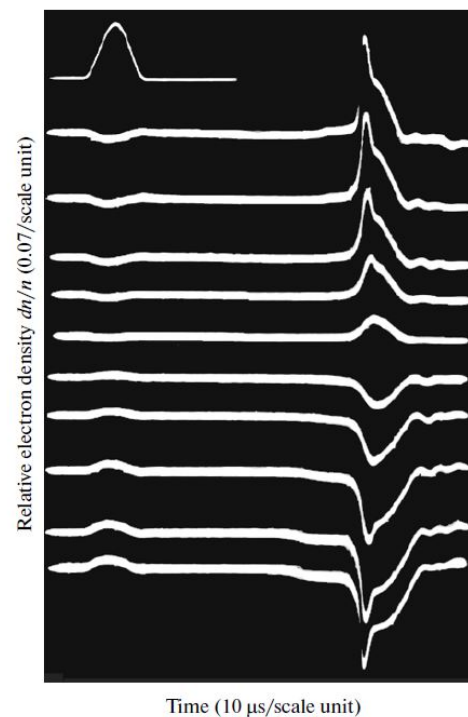


Fig. 1. Oscilloscope traces of the electron density in ion–acoustic solitons in SF₆–Ar plasma obtained at various excitation amplitudes; given at the top left is the profile of the excitation pulse; the top three and the bottom three traces have a clear angular shape (notations are as given in [11]).

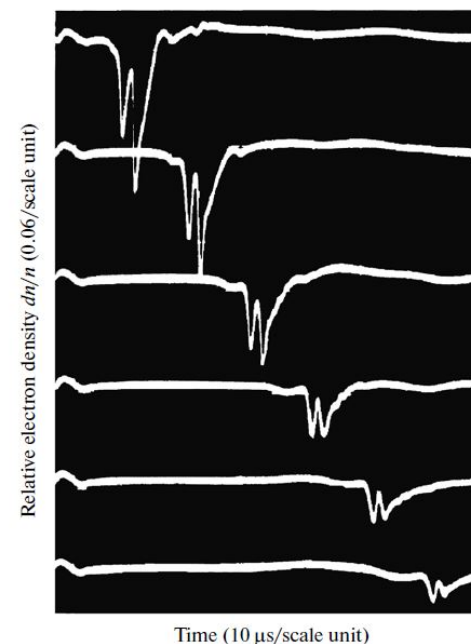


Fig. 2. Oscilloscope traces of the electron density in rarefactive ion–acoustic solitons in Ar–SF₆ plasma obtained at various distances from the excitation site, all the traces exhibit several pronounced minima (notations are as given in [10]).

where $e < 0$ is the charge of the electron and the negative ions; $(-e) > 0$ is the charge of the positive ions; all

Electrostatic supersolitons in three-species plasmas

Frank Verheest,^{1,2,a)} Manfred A. Hellberg,^{2,b)} and Ioannis Kourakis^{3,c)}
¹*Sterrenkundig Observatorium, Universiteit Gent, Krijgslaan 281, B-9000 Gent, Belgium*
²*School of Chemistry and Physics, University of KwaZulu-Natal, Durban 4000, South Africa*
³*Department of Physics and Astronomy, Centre for Plasma Physics, Queen's University Belfast, BT7 1NN Northern Ireland, United Kingdom*

(Received 13 December 2012; accepted 21 December 2012; published online 10 January 2013)

Superficially, electrostatic potential profiles of supersolitons look like those of traditional solitons. However, their electric field profiles are markedly different, having additional extrema on the wings of the standard bipolar structure. This new concept was recently pointed out in the literature for a plasma model with five species. Here, it is shown that electrostatic supersolitons are not an artefact of exotic, complicated plasma models, but can exist even in three-species plasmas and are likely to occur in space plasmas. Further, a methodology is given to delineate their existence domains in a systematic fashion by determining the specific limiting factors. © 2013 American Institute of Physics. [<http://dx.doi.org/10.1063/1.4775085>]

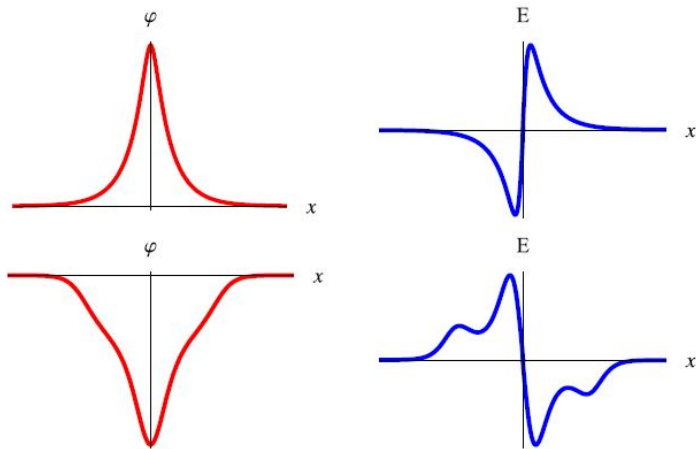


FIG. 1. *Upper panels:* Example of a standard positive soliton and its associated electric field. *Lower panels:* A negative supersoliton and its associated electric field.

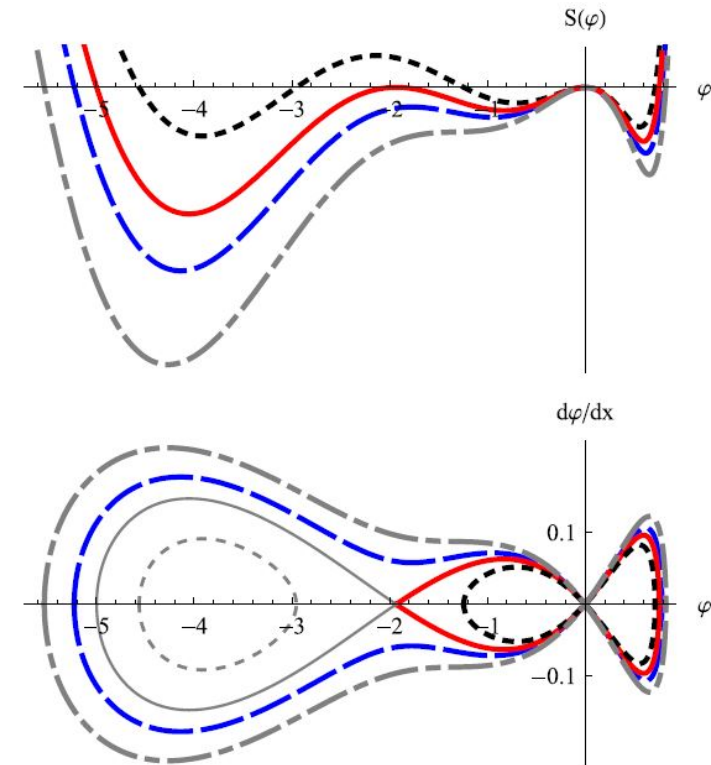


FIG. 3. *Upper panel:* Graphs of $S(\varphi)$ for $\beta = 0.3$, $\mu = 10$, $f = 0.3$ and $M/M_s = 1.023$ (dotted curve), $M/M_s = 1.027$ (solid curve), $M/M_s = 1.030$ (dashed curve) and $M/M_s = 1.035$ (dotted-dashed curve). *Lower panel:* Here the hodographs are presented, with the same curve coding. Thin dotted and solid curves in gray indicate ranges which are not accessible from the undisturbed conditions and thus physically irrelevant.

Dust-ion-acoustic supersolitons in dusty plasmas with nonthermal electrons

Frank Verheest*

Sterrenkundig Observatorium, Universiteit Gent, Krijgslaan 281, B-9000 Gent, Belgium & School of Chemistry and Physics, University of KwaZulu-Natal, Durban 4000, South Africa

Manfred A. Hellberg†

School of Chemistry and Physics, University of KwaZulu-Natal, Durban 4000, South Africa

Ioannis Kourakis‡

Centre for Plasma Physics, Department of Physics and Astronomy, Queen's University Belfast, BT7 1NN Northern Ireland, United Kingdom (Received 26 February 2013; published 15 April 2013)

Supersolitons are a recent addition to the literature on large-amplitude solitary waves in multispecies plasmas. They are distinguished from the usual solitons by their associated electric field profiles which are inherently distinct from traditional bipolar structures. In this paper, dust-ion-acoustic modes in a dusty plasma with stationary negative dust, cold fluid protons, and nonthermal electrons are investigated through a Sagdeev pseudopotential approach to see where supersolitons fit between ranges of ordinary solitons and double layers, as supersolitons always have finite amplitudes. They therefore cannot be described by reductive perturbation treatments, which rely on a weak amplitude assumption. A systematic methodology and discussion is given to distinguish the existence domains in solitary wave speed and amplitude for the different solitons, supersolitons and double layers, in terms of compositional parameters for the plasma model under consideration.

DUST-ION-ACOUSTIC SUPERSOLITONS IN DUSTY ...

PHYSICAL REVIEW E 87, 043107 (2013)

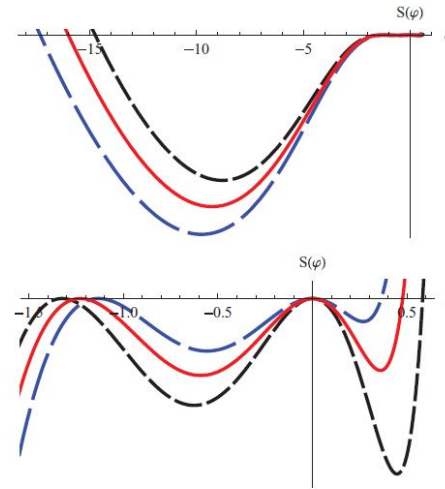


FIG. 4. (Color online) Upper panel: Pseudopotentials with a negative double layer for $f = 0.31$ (blue curve with longer dashes), $f = 0.320$ (red solid curve, at the precise polarity crossover), and $f = 0.33$ (black curve with shorter dashes). Lower panel: Focus on the φ range closer to the undisturbed conditions. Both panels together show that as f is increased, the absolute values of the large negative root decrease, whereas the amplitudes of the negative double layers and the positive soliton increase.

double layers. For a given value of f , the lower limit in M of the supersoliton existence domain is then governed by the

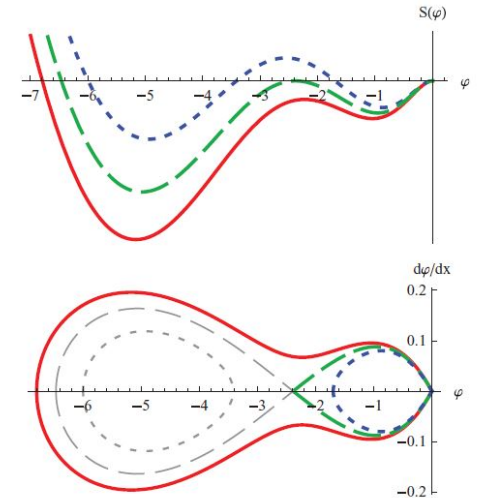


FIG. 5. (Color online) Upper panel: Pseudopotentials with a standard soliton (blue dotted curve, $M/M_s = 1.057$), a double layer (green dashed curve, $M/M_s = 1.061$), and a supersoliton (red solid curve, $M/M_s = 1.065$) for $\beta = 0.3$ and $f = 0.43$. For graphical clarity, the positive soliton domain has been omitted, because the well on this side is very deep and would flatten the important details on the negative side. Lower panel: Here the hodographs are presented, plotting $d\varphi/dx$ as functions of φ , with the same curve coding. Thin dotted and dashed curves in gray indicate ranges which are not accessible from the undisturbed conditions.

* From: NS Saint, I Kourakis and M Hellberg, PoP 16, 062903 (2009) |

Supersolitons in Space plasma observations?

- ESWs occur in abundance as magnetic-field aligned *bipolar* electric field structures (among other forms), observed in abundance in satellite data (Cluster, FAST, ...)
- Solitary waves: potential pulses, solitons, double layers, flat-topped pulses, ...

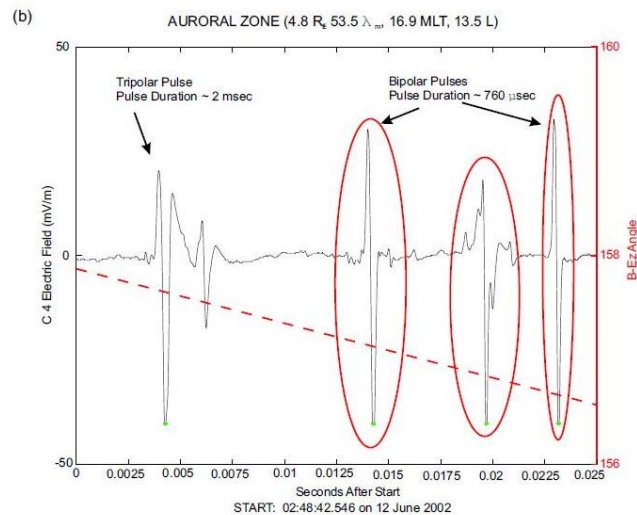


Fig. 1. Cluster WBD data taken on 12 June 2002 in the auroral zone. (a) Spectrogram showing the frequency and power spectral density of the emissions. The broad-band signals ranging up to about 10 kHz are indicative of times when IES are observed. (b) Representative waveform from a time of the broad-band signals, showing the two types of IES: bipolar and tripolar pulses.

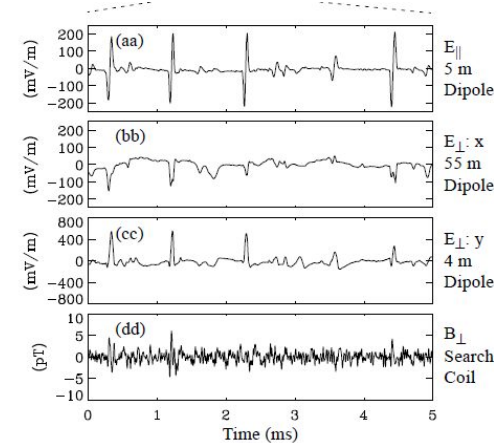


Figure 5. (From [5]) (a) The electric field parallel to B_0 . (b) The electric field perpendicular to B_0 (ΔE_{\perp}) and in the spin plane of the satellite. This signal, measured by a 56 m dipole antenna, appears attenuated, indicating that the structure size may have been < 112 m. (c) ΔE_{\perp} along the spin axis of the satellite. (d) A perturbation magnetic field perpendicular to B_0 (ΔB_{\perp}). ΔB_{\perp} was filtered to a pass band (3 kHz–16 kHz) to expose the weak signals and therefore may not appear unipolar in this figure. (aa)–(dd) An expanded view of this data.

Figures from: Pickett *et al* Ann. Geophys. (2004) (L, Cluster), Ergun *et al*, PPCF (1999) (R, FAST)

One-Dimensional Fluid Code

Plasma Model

(Fluid ions, cold & hot kappa distributed electrons)

$$\frac{\partial N_i}{\partial t_n} + \frac{\partial(N_i U_i)}{\partial x_n} = 0$$

$$\frac{\partial U_i}{\partial t_n} + U_i \frac{\partial U_i}{\partial x_n} = -\frac{\partial \Phi}{\partial x_n}$$

$$N_{he} = \left[1 - \frac{\Phi}{(\kappa_{he} - 3/2)} \right]^{-\kappa_{he} + 1/2}$$

$$N_{ce} = \left[1 - \frac{\Phi}{\tau(\kappa_{ce} - 3/2)} \right]^{-\kappa_{ce} + 1/2}$$

$$\frac{\partial^2 \Phi}{\partial x_n^2} = f N_{ce} + (1 - f) N_{he} - N_i$$

4th order finite difference scheme

Spatial derivative

4th order finite difference scheme

$$\frac{\partial F_h}{\partial x} = \frac{8(F_{h+1} - F_{h-1}) - F_{h+2} + F_{h-2}}{12\Delta x} \quad O(\Delta x)^4$$

$F_h \rightarrow$ represent a physical quantity defined at grid "h"
 $\Delta x \rightarrow$ Grid Spacing

Time derivative

Leap-frog method

$$\frac{\partial n}{\partial t} = f, \quad \frac{n(j+1,i) - n(j,i)}{\Delta t} = f(j+1/2,i) \quad O(\Delta t)^2$$

Here, $\Delta t \rightarrow$ Time step

Kakad, Omura & Kakad et al PoP, 2013

- (a) Memory allocation
- (b) Initialising N_i, N_e, U_i, Φ

INTEGRATING

- (1) Momentum equation of ions

$$U_i = - \int_{\Delta t} \left[U_i \frac{\partial U_i}{\partial x} + \frac{\partial \Phi}{\partial x} \right] dt$$

- (2) Continuity equation of ions

$$N_i = - \int_{\Delta t} \frac{\partial(N_i U_i)}{\partial x} dt$$

Δt

POISSON SOLVER

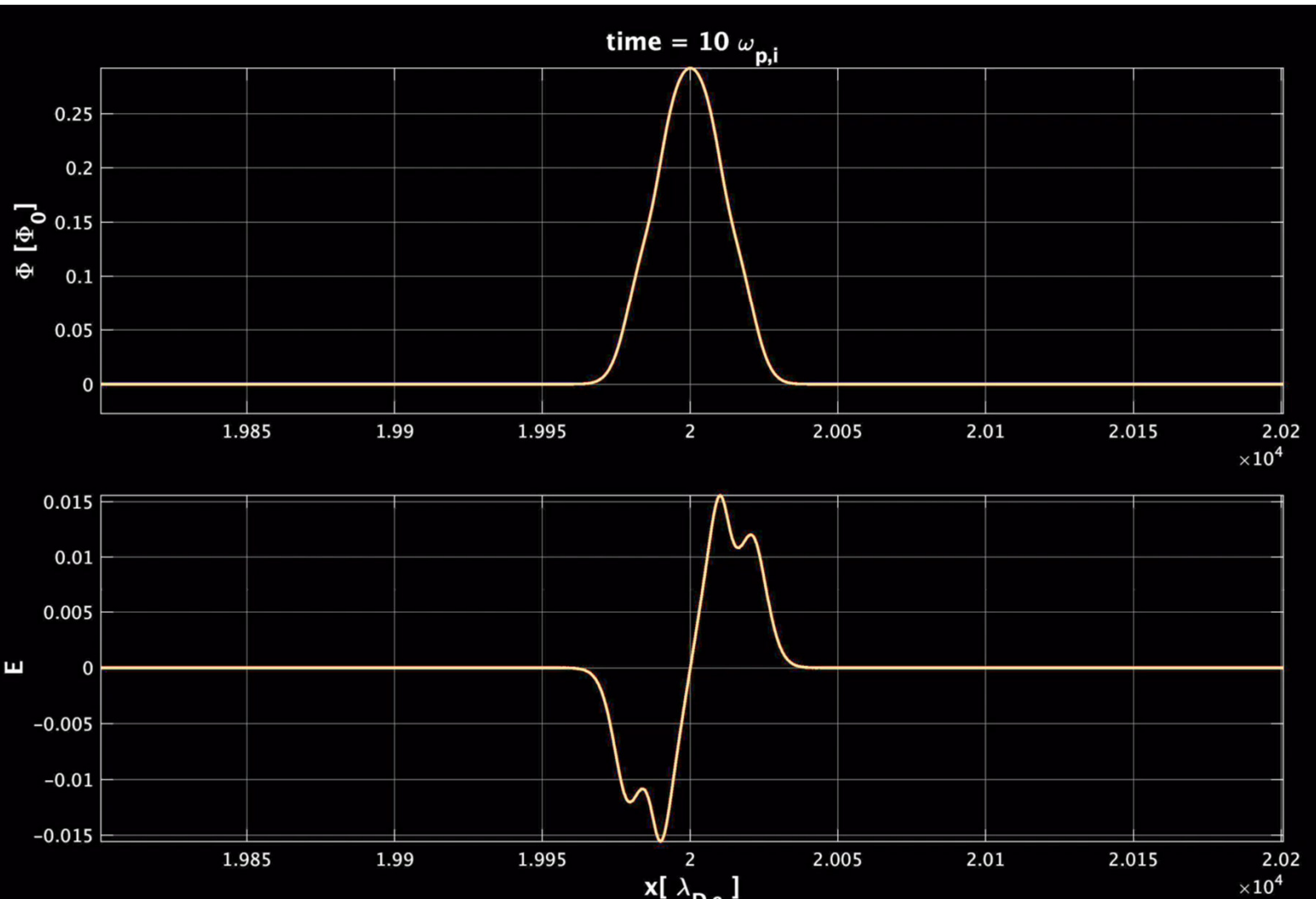
$$\Phi = \int_L \left[\int_L (N_e - N_i) dx \right] dx$$

$$N_e = \left[1 - \frac{\Phi}{\kappa - 3/2} \right]^{-\kappa + 1/2}$$

Successive Over Relaxation method best for simulating plasma with kappa distributions

Lotekar, Kakad, Kakad et al, CNSNS, 2019

Evolution of Supersolitons through density perturbation



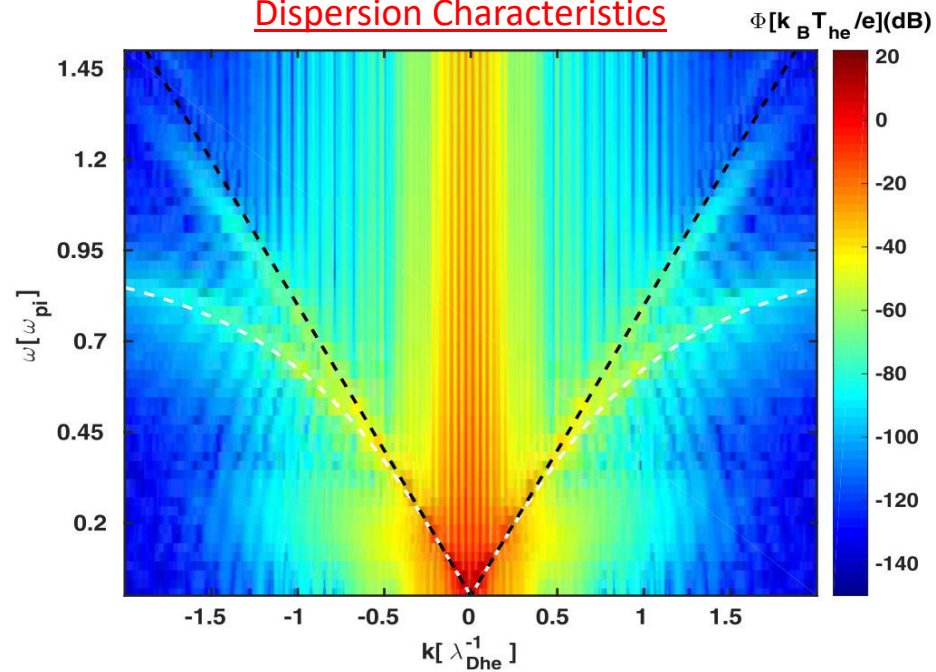
First-ever model simulation of the new subclass of solitons "Supersolitons" in plasma

Kakad+Lotekar+ Kakad,
Physics of Plasmas, 2016

->>> See movie 1 by Amar Kakad

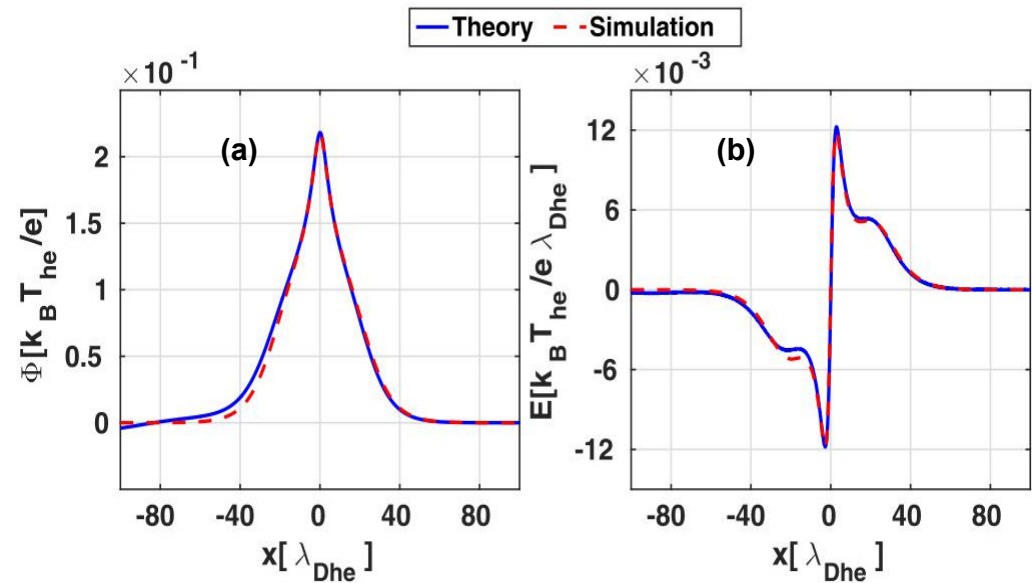
Supersolitons: Characteristics

Dispersion Characteristics



ω - k diagram during time = 0–200 from the simulation

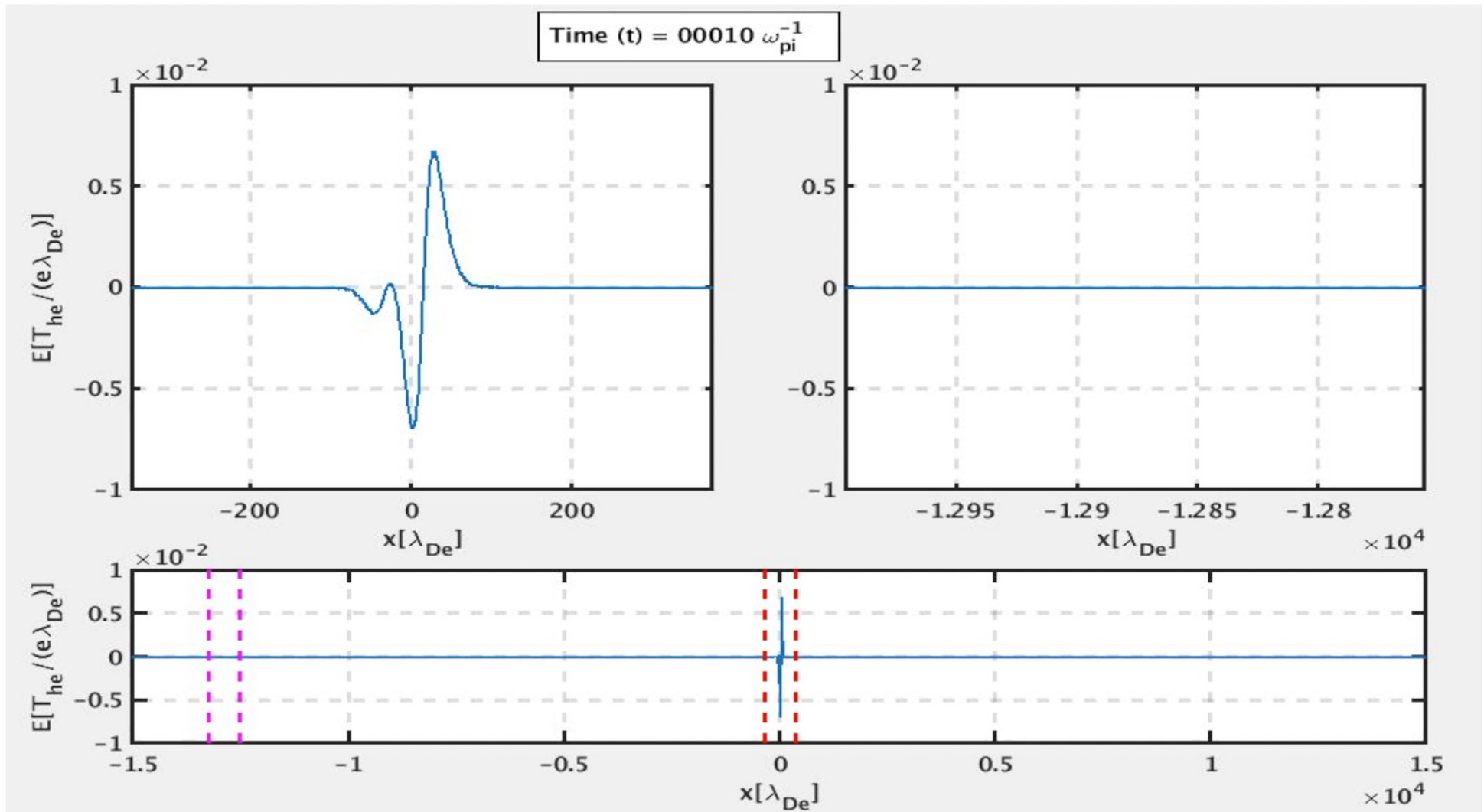
Simulation vs Theory



(a) potential (ϕ) and (b) electric field (E_n) profiles of IA supersoliton from simulation and theory

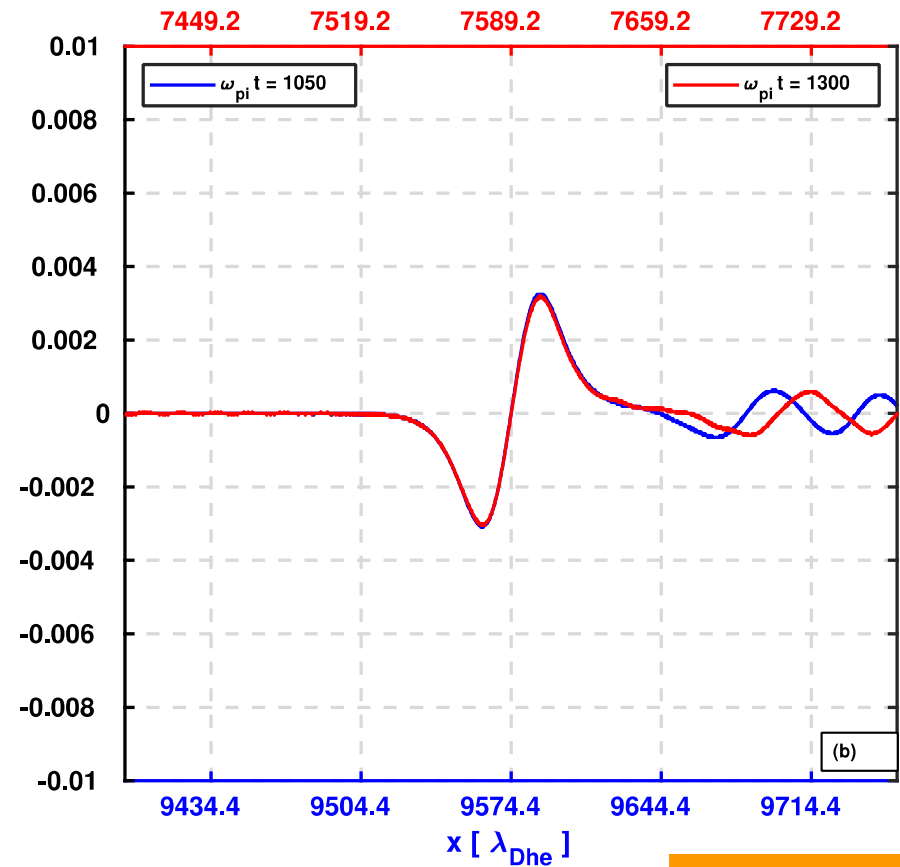
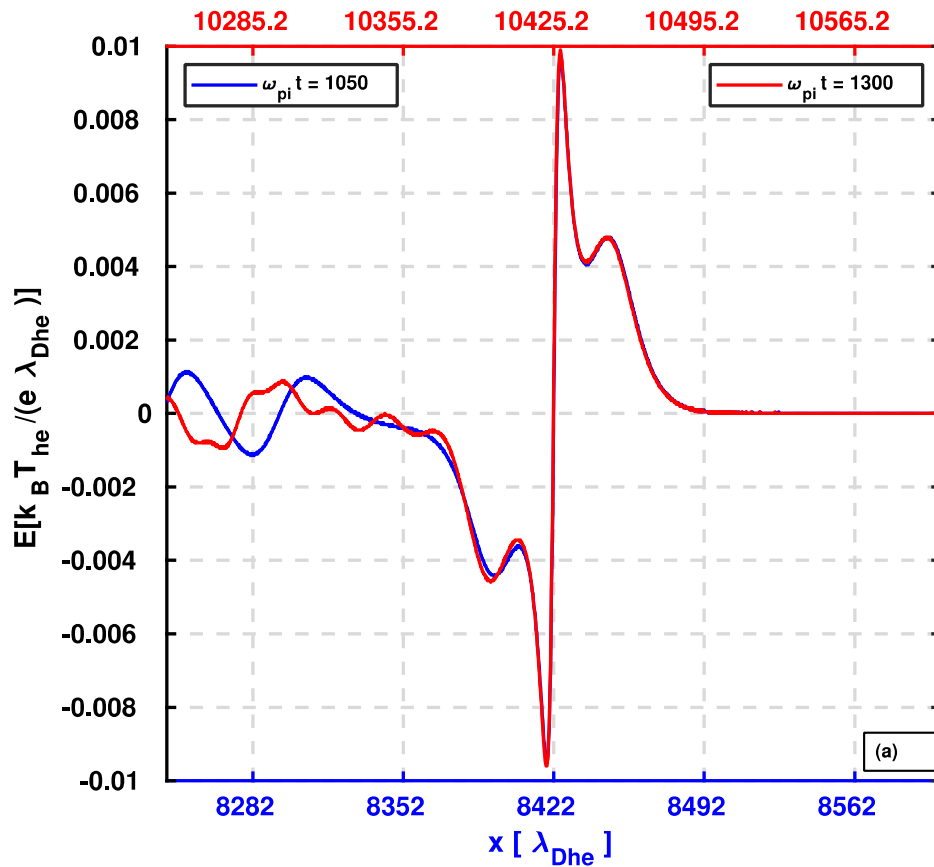
Collision of Supersolitons with Regular Soliton

Lotekar+Kakad+Kakad,
Physics of Plasmas, 2016



->>> See movie 2 by Amar Kakad

SSW and RSW before & after collision



Phase space holes in kinetic simulations

Method: Fully kinetic simulation approach based on the Vlasov-Poisson system:

Vlasov equation:

$$\frac{\partial f_j}{\partial x} + v \frac{\partial f_j}{\partial x} + \frac{q_j}{m_j} E \frac{\partial f_j}{\partial v} = 0$$

Poisson equation :

$$\frac{\partial^2 \varphi}{\partial x^2} = \frac{e}{\epsilon_0} (n_e - n_i)$$

In which f_j is the distribution function, \mathbf{E} and \mathbf{B} represent the electric and magnetic field.

Number densities:

$$n_j = \sum_{j=e,i} n_{0,i} \int f_j dv$$

in which i and e denote electron and ions respectively.

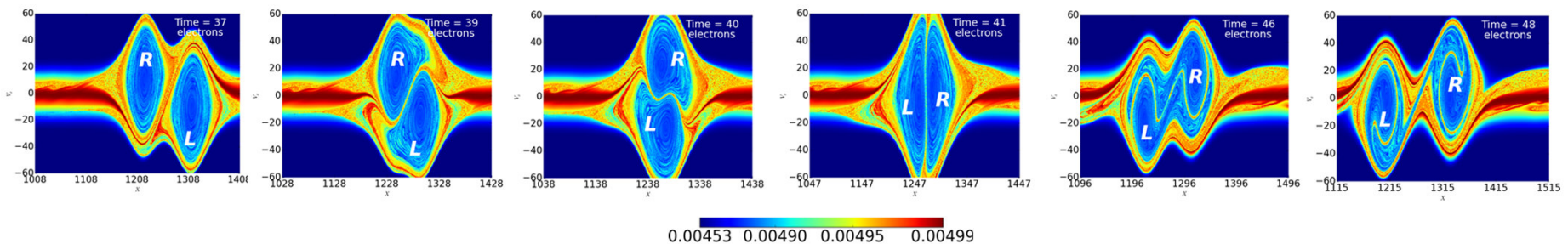
Electron Holes in the kinetic framework

- **Method:**

- Fully kinetic simulation approach based on Vlasov-Poisson equation

- **Findings:**

- 1. Electron holes accompanying solitons show strong resilience against mutual collisions.
- 2. In kinetic simulation is revealed that the internal structure of the electron hole changes after each collision without any traceable impact on the fluid-level characteristics such as density or its electrostatic feature such as electric field or potential

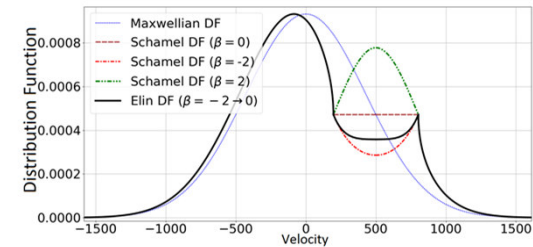


Source: SM Jenab Hosseini and F. Spanier, *Fully kinetic simulation study of ion-acoustic solitons in the presence of trapped electrons*, Physical Review E **95** 5 053201 (2017).

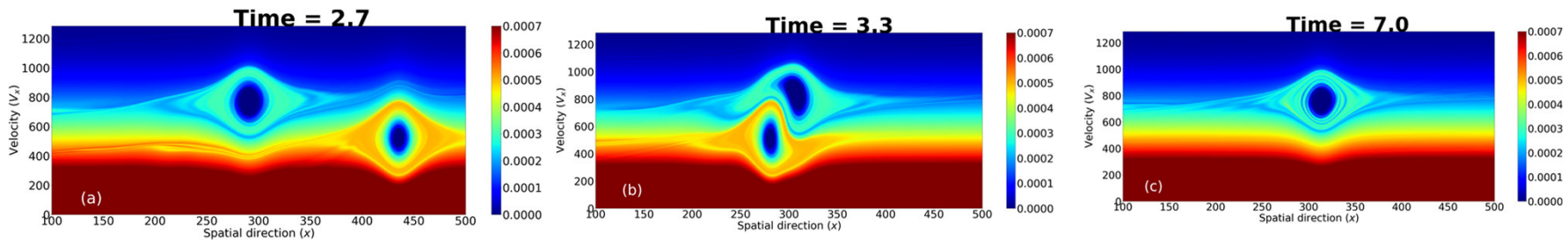
->>> See movies 1 & 2 by Mehdi Jenab

“Elin” Distribution Function for ultrafast electron holes

- Powerful simulation framework to study kinetic effects of hole and solitons
- The *Elin* df is proposed by generalizing the original Schamel df in a recursive manner.
- Adopting the *Elin* df, nonlinear solutions obtained by kinetic simulations with velocities twice the electron thermal speed coined as “Ultrafast electron holes”



Comparison of Elin DF with Maxwellian and Schamel DF




Overtaking collision of two ultrafast electron hole in the phase space

Source: SM Jenab Hosseini, G. Brodin, J. Juno & I. Kourakis, *Ultrafast electron holes in plasma phase space dynamics*, Scientific Reports, **11** (1), 1-9 (2021).

Article

Two-Parametric, Mathematically Undisclosed Solitary Electron Holes and Their Evolution Equation

Hans Schamel 

Physikalisches Institut, Universität Bayreuth, D-95440 Bayreuth, Germany; hans.schamel@uni-bayreuth.de

Received: 11 August 2020; Accepted: 25 September 2020; Published: 30 September 2020



Abstract: The examination of the mutual influence of the two main trapping scenarios, which are characterized by B and D and which in isolation yield the known sech^4 ($D = 0$) and Gaussian ($B = 0$) electron holes, show generalized, two-parametric solitary wave solutions. This increases the variety of hole solutions considerably beyond the two cases previously discussed, but at the expense of their mathematical disclosure, since $\phi(x)$, the electrical wave potential, can no longer be expressed analytically by known functions. Therefore, they belong to a variety with a partially hidden mathematical background, a hitherto unexplored world of structure formation, the origin of which is the chaotic individual particle dynamics at resonance in the coherent wave particle interaction. A third trapping scenario Γ , being independent of (B, D) and representing the perturbative trapping scenarios in lowest order, provides a broad, continuous band of associated phase velocities v_0 . For structures propagating near $C_{SEA} = 1.307$, the *slow electron acoustic speed*, a Generalized Schamel equation is derived: $\varphi_\tau + [\mathcal{A} - B\frac{15}{8}\sqrt{\varphi} + D \ln \varphi]\varphi_x - \varphi_{xxx} = 0$, which governs their evolution. \mathcal{A} is associated with the phase speed and $\tau := C_{SEA}t$ and $\varphi := \phi/\psi \geq 0$ are the renormalized time and electric potential, respectively, where ψ is the amplitude of the structure.

Additional slides for plasma and simulation parameters

Plasma and Simulation Parameters for generation of supersoliton (slides 2&3)

Initial Perturbation Form: Gaussian Potential

$$n_j = n_{j0} + \Delta n \text{Exp} \left[- \left(\frac{x - x_c}{l_0} \right)^2 \right]$$

Here, Δn is the amplitude of the perturbation, x is the position on the x -axis, x_c is the center of the system, and l_0 controls the width of the perturbation.

Simulation Parameters: $\Delta n = 1.9 n_{i0}$ and $l_0 = 10 k \lambda_{dhe}$, Grid spacing: $\Delta x = 0.2 k \lambda_{dhe}$,

time interval: $\Delta t = 0.1 \omega_{pi}^{-1}$, and system length: $Lx = 40000 k \lambda_{dhe}$.

Plasma Parameters: $f = 0.055$, $\tau = 0.12$, $\kappa_{ce} = 10$, and $\kappa_{he} = 10$

(Verheest, Hellberg & Kourakis PoP 2013)

The flow velocities of the plasma species at $t = 0$ are assumed to be zero

Plasma and Simulation Parameters: Head-on collision of supersoliton with regular soliton

Perturbation used: In both densities and in ion velocity

$$n_s(x) = \begin{cases} n_{s0} \left(1 + \Delta n_s \exp \left[- \left(\frac{x-x_{ssw}}{l_{n0}} \right)^2 \right] \right), & \text{if } \omega_{pi} t = 0. \\ n_{s0} \left(1 + \Delta n_s \exp \left[- \left(\frac{x-x_{rsw}}{l_{n0}} \right)^2 \right] \right), & \text{if } \omega_{pi} t = 1100. \end{cases}$$

$$U_i(x) = \begin{cases} \Delta v_s \exp \left[- \left(\frac{x-x_{ssw}}{l_{v0}} \right)^2 \right] & \text{if } \omega_{pi} t = 0. \\ -\Delta v_s \exp \left[- \left(\frac{x-x_{rsw}}{l_{v0}} \right)^2 \right], & \text{if } \omega_{pi} t = 1100. \end{cases}$$

TABLE I. The perturbation parameters used for the generation of SSW and RSW in the simulation.

Perturbation		SSW	RSW	Normalizing unit
Density (s=we, he, i)	Δn_s	0.32	0.2	n_{0i}
	l_{n0s}	31	10	λ_{Dhe}
Velocity (s=i)	Δv_s	0.4	-0.1	C_{IA}
	l_{v0s}	20	20	λ_{Dhe}
Position	x_0	0	-12875	λ_{Dhe}
Time	t	0	1070	ω_{pi}^{-1}

Plasma Parameters: $f = 0.055$, $\tau = 0.12$, $\kappa_{ce} = 10$, and $\kappa_{he} = 10$
(*Verheest, Hellberg & Kourakis PoP 2013*)

Flow velocities of plasma species at $t = 0$ are assumed to be zero